Republic of Iraq
Ministry of Higher Education
and Scientific Research
University of Al-Qadisiayh
College of Education
Department of Physics

Investigation On The Performance Of Lithium Triborate (LBO) Crystal For Higher Harmonics Generation of LASERS

A Thesis
Submitted to The Council of the College of Education, University of Al-Qadisiayh in Partial Fulfillment of the Requirements
For the Degree of Master of Science in Physics

by

Zahraa Sahib Shanon

B.Sc. in Physics 2013 - University of Al-Qadisiayh

Supervised by:

Prof. Dr. Raad Sh. Alnayli   **Prof. Dr. Khawla J. Tahir**

2016 A.D.   1437 A.H.

بِسْمِ اللهِ الرَّحْمنِ الرَّحِيمِ

اللَّهُ نُورُ السَّمَاوَاتِ وَالْأَرْضِ مَثَلُ نُورِهِ كَمِشْكَاةٍ فِيهَا مِصْبَاحٌ الْمِصْبَاحُ فِي زُجَاجَةٍ الزُّجَاجَةُ كَأَنَّهَا كَوْكَبٌ دُرِّيٌّ يُوقَدُ مِنْ شَجَرَةٍ مُبَارَكَةٍ زَيْتُونَةٍ لَا شَرْقِيَّةٍ وَلَا غَرْبِيَّةٍ يَكَادُ زَيْتُهَا يُضِيءُ وَلَوْلَمْ تَمْسَسْهُ نَارٌ نُورٌ عَلَى نُورٍ يَهْدِي اللَّهُ لِنُورِهِ مَنْ يَشَاءُ وَيَضْرِبُ اللَّهُ الْأَمْثَالَ لِلنَّاسِ وَاللَّهُ بِكُلِّ شَيْءٍ عَلِيمٌ ﴿٣٥﴾

صدق الله العلي العظيم

الآية (٣٥) من سورة النور

DEDICATION

To My Great Teacher

Prophet Mohammed And His Progeny (PBUT)

To Those Whom I Owe My Life

My Family, Specially My Father

To The People Who Paved Our Way Of Science And

Knowledge

All Our Teachers Distinguished

I Submit This Modest Work

Zahraa

Acknowledgments

In the name of Allah, the most beneficent, the most Merciful. All praise and thank to Allah, the Lord of the universe and all that exists, Who taught me what I don't know, Who inspired me, and nurtured my powers of observation and reasoning. Prayers and peace be upon His prophet, Mohammed , and his progeny , the last messenger for all mankind .

First, I would like to express my deepest thanks and appreciation to My supervisor, *Prof. Dr. **Raad Shaker Obiss Alnayli** and Prof. Dr. **Khawla jameel Tahar***, for their patience, support, and guidance throughout my research period. It has been a great pleasure for me to be one of their students. Their deep understanding of physics with both fundamental and applied science has inspired me most.

My extreme love and appreciation to my Father *Prof. Dr. **Sahib Shanon Ibraheim*** for his moral support, long suffering and patience during my study.

The grateful is extended to the staff of the College of Education and the Department of Physics in Al-Qadisiayh University for all assistance, support, and guidance .

My thanks are extended to ***Hawraa H. AL-Ghanemy*** in University of Karbala for her help and support in my thesis.

Finally, I would like to say 'thank you' to *Prof. Dr. Fadhil I. Sharrad* the Head of the Department of Physics in the College of Sciences-University of Karbala for his help.

Zahraa

Supervisor Certificate

We certify that this thesis (Investigation On The Performance of Lithium Triborate (LBO) Crystal For Higher Harmonics Generation of LASERS) by (Zahraa Sahib Shanon) was prepared under our supervision at the Department of physics, College of Education, University of al-Qadisiayh, in partial requirement for the degree of Master of Science in physics.

Signature

Prof. Dr. Raad Shaker Alnayli

University of al-Qadisiayh
College ofEducation
Department of physics
(Supervisor)
Date: 27 / 7 /2016

Signature

Prof. Dr. Khawlajameel Tahir

University of Karbala
College of Sciences
Department of physics
(Supervisor)
Date: 27 / 7 /2016

In view of the available recommendations, I forward this thesis for debate by the examination committee.

Signature

Asst. Prof. Abdulhussain Abbas Khiedyer

(Head of the Department of physics)

Date: 27 / 7 /2016

Examining Committee Certification

We, the member of examining committee, certify that we have read this thesis entitled *"Investigation On The Performance of Lithium Triborate (LBO) Crystal For Higher Harmonics Generation of LASERS"* and examined the student "Zahraa Sahib Shanon" in its contents and that, in our opinion it is adequate for the partial fulfillment of the Requirements for the degree of Master of Science in Physics.

Signature

Name : Prof. Sahib Nama Abdul-wahid

Address : University of Kufa, Faculty of Education
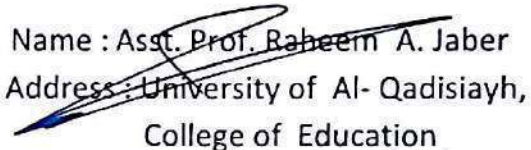
Date :

(Chairman)

Signature

Name : Asst. Prof . Falah H.Hanaon

Address : University of Thi-Qar,
College of science

Date :

(Member)

Signature

Name : Asst. Prof. Raheem A. Jaber

Address : University of Al- Qadisiayh,
College of Education

Date : 29-12-2016

(Member)

Signature

Name : Prof. Raad Sh. Alnayli

Address : University of Al-Qadisiyah,
College of Education

Date :

(Member and Supervisor)

Signature

Name : Prof. Khawla J. Tahir

Adress : University of Karbala,
College of Sciences

Date :

(Member and Supervisor)

Approved by the Deanery of the College of Education

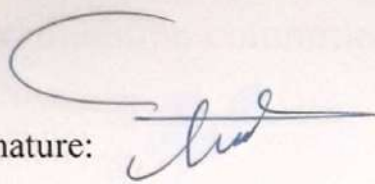Signature

Name : Prof. Dr. Khalid Jawad Kadhim Al-Adilee

Rank: Professor

Position: Dean of College of Education

Date: 8/ 1/ 2017

Certification of Linguistic Evaluation

I Certify that thesis entitled *"Investigation On The Performance of Lithium Triborate (LBO) Crystal For Higher Harmonics Generation of LASERS* " by the student *"Zahraa Sahib Shanon* " was evaluated linguistically, and I forward it debate by the examination committee.

Signature:

Name: Habeeb M. A. AL-Saeedi

Title: Asst. Lecturer

Address: Department of English , University of al-Qadisiayh, College of Education

Date: 7/9/2016

Contents

List of contents

Abstract

In this thesis, harmonics generation, the linear and nonlinear optical properties have been studied experimentally to optimize the performance of the single pure Lithium Triborate (LBO) crystal which has dimensions $(5.95 \times 5.95 \times 5.95)$ mm^3 as proposal element model for the combination of the harmonics generation using Nd:YAG laser has the fundamental spectral wavelengths about 1064 nm and 532 nm.

The LBO crystal has been subjected to UV-Visible spectrophotometer to measure the absorption spectra and the Transmission spectra, to calculate the linear absorption coefficient and linear refractive index. Then, the nonlinear optical properties described by nonlinear absorption coefficient and nonlinear refractive index are calculated using a highly sensitive method known as Z-Scan Technique.

Z-Scan Experiment was performed using CW Nd:YAG laser with the power output of 25and 40 mW in the two common parts as, the first part has been done using a closed aperture put in front of the detector to measure the nonlinear refractive index at two wavelengths (1064nm and 532nm). For 1064nm wavelength, the nonlinear refractive index is found to be $n_2 = 0.62 \times 10^{-9}$ cm^2/ mW at output power (40 mW). For 532nm wavelength, the nonlinear refractive index is found to be $n_2 = 3.04 \times 10^{-9}$ cm^2/ mW at output power (25 mW) and $n_2 = 1.85 \times 10^{-9}$ cm^2/ mW at output power (40 mW). Then, the aperture was removed and this technique called the open aperture Z-Scan to measure the nonlinear absorption coefficient at two wavelengths (1064nm and 532nm). Also, for two different applied powers at 532nm. For 1064nm wavelength the nonlinear absorption coefficient is found to be $\beta = 2.3 \times 10^{-3}$ cm/mW. For 532nm wavelength, the nonlinear absorption coefficient is found to be

$\beta = 3.7 \times 10^{-3}$ cm/ mW at output power (25 mW) and $\beta = 2.3 \times 10^{-3}$ cm/ mW at output power (40 mW).

The experimental results for closed aperture Z-Scan showed that the LBO crystal exhibits positive refractive index (self-focusing). For open aperture Z-Scan the results showed that the crystal exhibited saturation absorption in the wavelength 532 nm.

The ability to obtained third harmonics in Lithium Triborate (LBO) crystal has been arranged using the range of powers (90-130) mW of CW Nd:YAG laser. The possibility of generation these signals of third harmonics generation has been detected using Laser Power Meter.

Dependence the harmonics generation on the intensity has been determined at two cases with variable input power laser(80mWand 35mW). The minimum values of threshold incident intensity to obtain THG intensity are equal $I_{3\omega} = 7.33 \times 10^9$ mW/cm^2 at 157269 mW/cm^2 and $I_{3\omega} = 1.04 \times 10^9$ mW/cm^2 68805 mW/cm^2 input power intensity.

The rough estimated of the conversion efficiency of 70% was achieved from the third harmonics generation by two steps arrangement of the obtainable UV laser beam and 30% was achieved from second harmonics generation at input power 80 and 35 mW, which is well agreement with the detector measurements owing to the efficiency of second harmonics generation were only one-two of the efficiency of third harmonics generation as well as the intensive laser most be applied. These results are very satisfactory apply this proposal model as optimum controlling element for the combined application as, the third harmonics generation(THG) and its second harmonics generation (SHG) at 1064nm.

List of symbols

Symbol	Definition	Unit
n	The refractive index of the material	-
n_o	The refractive index for the fundamental in the linear polarization	-
n_2	The non- linear refractive index	cm^2/mW
α	The absorption coefficient	cm^{-1}
α_o	The linear absorption coefficient	cm^{-1}
β	The nonlinear absorption coefficient	cm/mW
I	The incident intensity	mW/cm^2
P	The polarization of the material	$Coul./m^2$
E	The electric field strength	V/m
ε_o	The permittivity of vacuum	F/m
χ	The electric susceptibility of the medium	-
$\chi^{(1)}$	The linear susceptibility	-
$\chi^{(2)}$	The second nonlinear susceptibility	m/V
$\chi^{(3)}$	The third nonlinear susceptibility	m^2/V^2
$\mathbf{n_2}$	The refractive index for the fundamental the extraordinary polarization	-
n_3	The refractive index for the second harmonics in the extraordinary polarization	
d_{eff}	The Nonlinear coefficient	pm/V
Θ, Φ	The Cutting angles	Deg.
ρ	The Walk-off angle	rad.
λ	The wavelength	nm

h	Plank Constant	$m^2\ kg\ /\ s$
$P^{(3)}(3\omega)$	The third-order nonlinear polarization	$Coul./cm^2$
Re $\chi^{(3)}$	The real part of the third order nonlinear optical susceptibility	cm^2/W
Im $\chi^{(3)}$	The imaginary part of the third order nonlinear optical susceptibility $\chi^{(3)}$	cm^2/W
c	The speed of light	m/sec
ω	The angular frequency	rad.
p	The momentum	Kg.m/cm
k	The wavenumber	m^{-1}
ΔK	The phase matching	-
$k_{2\omega}$	The wave-vector of the second harmonics beam	mm^{-1}
k_{ω}	The wave vector of the fundamental beam	mm^{-1}
L_c	The coherence length	μm
Δk	The wave vector phase mismatch	-
q	The harmonics order	-
k_q	The wave vector of the qth harmonic	-
T(z)	The normalized transmittance	-
T_p	Normalized crystal transmittance when situated at the position of maximum transmittance (peak)	-
T_v	Normalized crystal transmittance when situated at the position of minimum transmittance (valley)	-
z	The position was obtained by moving the samples along the axis of the incident beam (z-direction) with respect to the focal point	mm
ΔT_{p-v}	The difference between the normalized peak and valley transmittance	mW

$\Delta\Phi_o$	The variation of phase distortion	rad.
I_o	The intensity of the laser beam at the focus	mW/cm^2
w_o	The beam radius at the focal point	mm
p	The power of laser beam	mW
L_{eff}	The effective thickness of the crystal	cm
t	The thickness of the crystal	mm
T	The transmittance	-
z_o	Rayleigh length	mm
ΔT	The one peak value at the open aperture Z-scan curve	mW
R	The reflectance	-
K	The extinction coefficient	-
A	The absorbance	-
σ	The optical conductivity	-
ε	The dielectric constant	-
ε_1	The real parts of the dielectric constant	-
ε_2	The imaginary parts of the dielectric constant	-
η_{SHG}	The conversion efficiency of second-harmonic generation	-
$I_{3\omega}$	The intensity of third harmonics generation beam	mW/cm^2
I_{ω}	The intensity of the input beam at frequency ω	mW/cm^2
L	Crystal length	mm
Ω_3	The efficiency of the conversion of a fundamental into third harmonics generation	-

List of Abbreviations

Abbreviation	Meaning
NLO	Nonlinear Optics
KDP	Potassium Dihydrogen Phosphate
BBO	β-Barium Borate
LBO	Lithium Triborate
HG	Harmonics Generation
SHG	Second Harmonics Generation
KTP	Potassium Titan Phosphate
Nd:YAG	Neodymium : Yttrium Aluminum Garnet
THG	Third Harmonics Generation
HHG	High Harmonics Generation
EUV	Electromagnetic Ultra-Violate
OPO	Optical Parametric Oscillation
FC	Frequency Conversion
QPM	Quasi-Phase Matching
SFG	Sum Frequency Generation
NCPM	Noncritical Phase Matching
CARS	Coherent Anti Stokes Raman Scattering
TPA	Two Photon Absorption
UV	Ultra-Violate
CW	Continuous Wave
LPM	LASER Power Meter

List of Figures

List of Tables

CHAPTER ONE

INTRODUCTION

AND

PREVIOUS WORKS

1.1 Introduction

This chapter contain the definition of Nonlinear Optics, It describes the types of harmonics generation and explain the process of nonlinear optics such as parametric oscillation, frequency conversion and phase matching.

1.2 Nonlinear Optics

Nonlinear optics (NLO) are the study of all the phenomena that occur from the interaction of light like the laser with matter [1,2]. The interaction of intensity light such as laser with a nonlinear optical material causes a modification of the optical properties of the system, and the next photon that arrives show a different material. Typically only laser light is sufficiently intense to generate NLO phenomena; therefore the beginning of this research field is taken to be the discovery of second-harmonics generation by Franken *et al.*(1961) [3], the year after the construction of the first laser by Maiman (1960) [4].

Although the observation of most nonlinear optical phenomena requires laser radiation, some classes of nonlinear-optical effects were known since a long period of time before the discovered of the laser. The most prominent examples of such phenomena include Pockel's and Kerr electro optic effects[5]. The theory of nonlinear optics builds on the well-understood theory of linear optics, particularly that part known as the interaction of light with matter. Ordinary matter consists of a collection of positive charged cores (of atoms or molecules) and surrounding negative charged electrons Light interacts primarily with matter via the valence electrons in the outer shells of electron orbitals. The fundamental parameter in this light-matter interaction theory is the electronic polarization of the material induced by light [6].

For instance, it has been observed that the linear behavior found in Snell's and Beer's law optical consider to be the laws to derive the optical behavior of many materials at high light intensities. In general, the refractive index (n) and the main absorption coefficient (α) are depend on the electric field of the laser light intensity [7].

$$n = n_o + n_2 I \ldots\ldots\ldots\ldots\ldots\ldots\ldots\ldots\ldots\ldots\ldots\ldots\ldots\ldots\ldots\ldots\ldots(1.1)$$

$$\alpha = \alpha_o + \beta I \ldots\ldots\ldots\ldots\ldots\ldots\ldots\ldots\ldots\ldots\ldots\ldots\ldots\ldots\ldots(1.2)$$

Where, I : is the incident intensity of laser light, n_o : is the refractive index for the fundamental in the linear polarization, n_2 : is the nonlinear refractive index, α_o : is the linear absorption coefficient and β :is the nonlinear absorption coefficient.

The nonlinear effect include interact between the beam of light and matter, which leads to make the electrons of the atoms in the material acting as electric dipoles. The light radiation interacts with the dipoles causing them to oscillate. The classical laws of electromagnetism results in the dipoles that acts as sources of light radiation. The phase velocity and wavelength of this electromagnetic wave are determined by the refractive index of the doubled angular frequency. The condition to obtain maximum values of conversion efficiency, is that the phase vectors of input and generated light beams are to be matched. If the amplitude of vibration is small, the dipoles emit radiation of the same frequency as the incident radiation.[8]

Typically the electric field is weak to not make the effects notice[9]. Compare with the case when the electric field strength is high the nonlinear reaction of some materials can be very large. Some crystals such as, Potassium Dihydrogen Phosphate (KDP), Beta Barium Borate (BBO) and lithium triborate (LBO) crystal, have strong nonlinearity and high damage threshold [9]. The material can be expanded into a Taylor

series when the electric field of this material is polarized and have high energy enough. So the polarization (P) can be express by[10]:

$$P = \varepsilon_o\left[\chi^{(1)}E + \chi^{(2)}E^2 + \chi^{(3)}E^3 + \cdots\right]\ldots\ldots\ldots\ldots\ldots\ldots\ldots\ldots(1.3)$$

Where: E: is the electric field strength, ε_o : is the permittivity of vacuum, $\chi^{(1)}$: is a linear susceptibility, $\chi^{(2)}$: the second nonlinear susceptibility, $\chi^{(3)}$: the third nonlinear susceptibility. And χ term responsible of the linear absorption and refraction, which is the only term that reflects the linear polarization and electric field.

The first term in equation (1.3) refers to the linear polarization response of the material. But with higher electric field strengths the other terms refer to nonlinear will also be large enough to make a contribution [5]. The electric polarization (P) almost linearly proportionally with the electric field when the applied electric field small enough [8], as:

$$P = \varepsilon_o \chi E \ldots\ldots\ldots\ldots\ldots\ldots\ldots\ldots\ldots\ldots\ldots\ldots\ldots\ldots\ldots\ldots\ldots\ldots\ldots(1.4)$$

Where : χ : electric susceptibility of the medium expresses the interaction between matter with light [11], on the other hand, the nonlinear dielectric medium is characterized by a nonlinear relation between P and E as illustrated in Fig. (1.1):
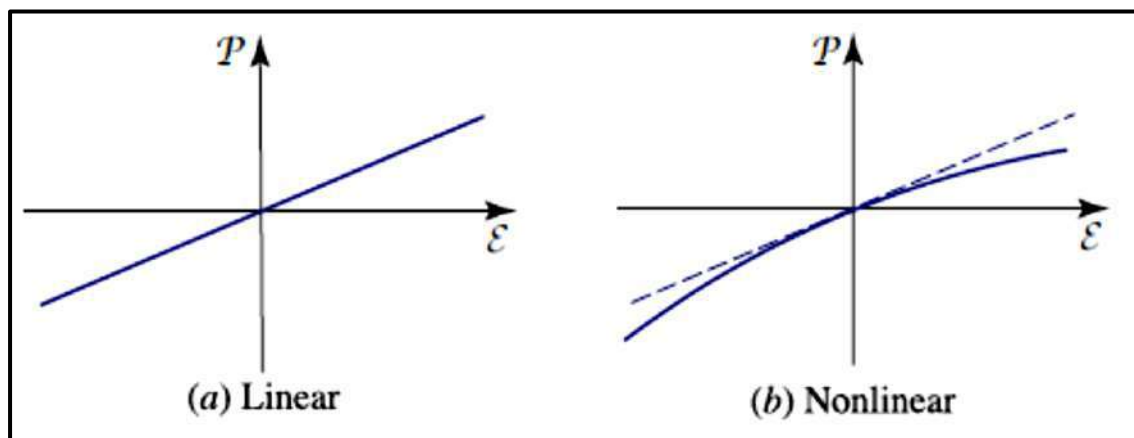
Figure (1.1) The P–E relation for (a) a linear dielectric medium, and (b) a nonlinear medium [12].

1.3 Descriptions of Nonlinear Optical Processes

Some of nonlinear optical processes are important to physicists, chemists, and other scientists because they are in common use in the laboratories, Such as harmonics generation, optical parametric oscillation and frequency conversion [8]:

1.3.1 Harmonics Generation (HG)

The generation of harmonics from laser light consider to be one of the most important nonlinear optical processes for technical applications, such as the main applications of nonlinear optics. Here we will discuss Second Harmonics Generation that used for producing visible and near ultraviolet coherent light, and the generation of higher harmonics.

1.3.1.1 Second Harmonics Generation (SHG)

Second Harmonics generation (SHG) was the first experiment in the history of nonlinear optics discovered by Franken *et al.* [13] soon after the invention of the Ruby laser [4].

The process occurs within a nonlinear medium, usually a crystal (KDP-Potassium di hydrogen phosphate, KTP-Potassium Titanyl Phosphate, etc.), Frequency doubling processes are commonly used to produce green light (532nm) using, a Nd:YAG (Neodymium: Yttrium Aluminum Garnet) laser operating with wavelength 1064 nm [8].

Second harmonics generation (SHG), in otherwise called "frequency doubling", is a process which converts light of one particular angular frequency to light at exactly double that frequency. Another way of saying it is to say that the wavelength is halved. This process only takes place under very specific conditions within a material which has a "second order non-linear" characteristic[13]. Materials of this kind are sometimes called chi-squared ($\chi^{(2)}$) materials. It can be produced double angular frequency by doubling the energy. Thus two photons of a

particular energy (and frequency) are combined (through interaction with a material) to give out a third photon containing all the energy of the original two (at double the frequency). Chemical bonds between pairs of atoms (called dipoles) resonate at particular frequencies (wavelengths, energy levels)[14].

The process of second harmonics generation involves the interaction of two waves at angular frequency ω to produce a wave with the angular frequency 2ω [15]. It is schematically illustrated in Fig. (1.2) below.
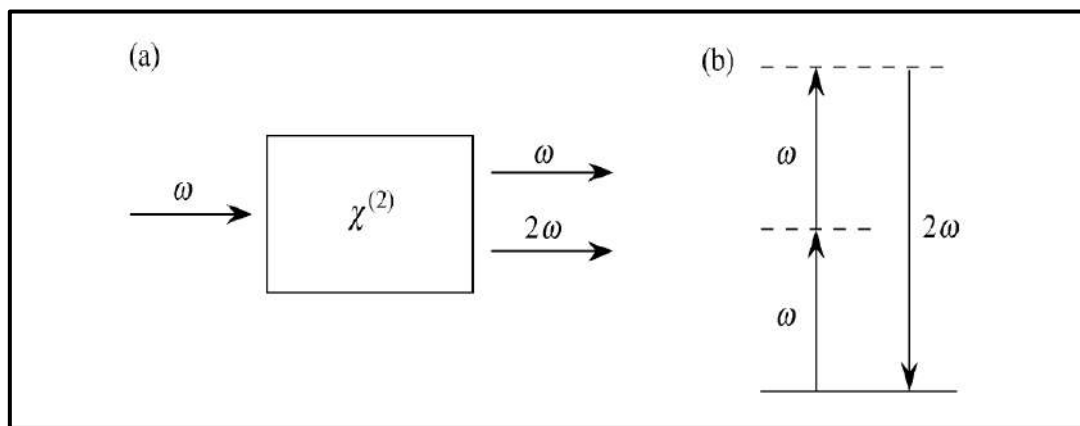
Figure (1.2) (a) Geometry of second-harmonics generation. (b) Energy-level diagram describing second-harmonics generation [1].

Figure (1.2), explains that the energies of the two absorbed photons aren't the same. This is the general case of "three-wave mixing" where a third photon with the sum of the energies of the original photons are produced from the interaction of two photons combine with a material. So, we have two photons with the same energy level combining to produce a third with the sum of the energies of the two original photons in the case of SHG [1], as is it seen in Fig. (1.3).
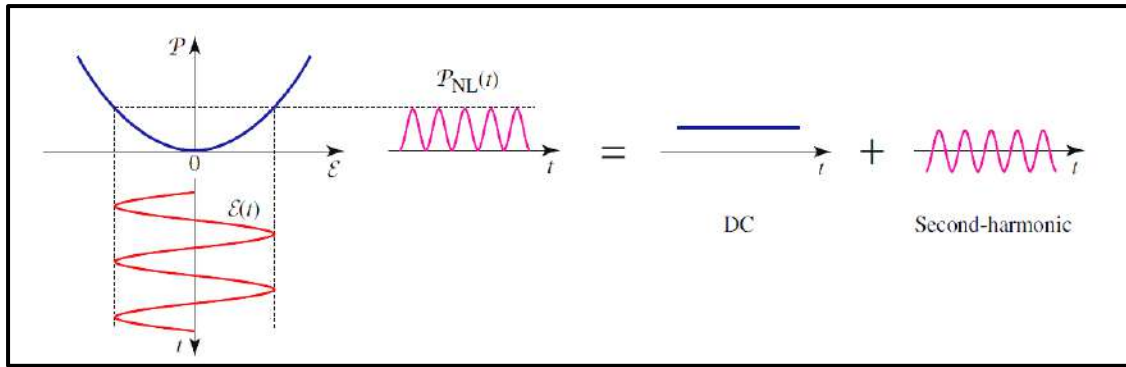
Figure(1. 3) A sinusoidal electric field of angular frequency ω in a second-order nonlinear optical medium creates a polarization with a component at 2ω (second-harmonics) and (dc) a steady component [12].

Since the emissions are added coherently, the intensity of the second harmonics wave is proportional to the square of the length of the effective volume L [16].

The phase matching condition for second harmonics generation becomes:[9]

$n_o + \mathbf{n_2} = 2n_3$ …………………………………………………………..(1.5)

Here $\mathbf{n_2}$ is the refractive index for the fundamental extraordinary polarization, and n_3 is the refractive index for the second harmonics extraordinary polarization. Table (1.1) explain the properties of LBO crystal in SHG.

Table (1.1) properties of LBO for the SHG from 798nm to 399 nm [17].

Parameter		
Nonlinear coefficient	d_{eff}	0.75 pm/V
Cutting angles	θ	90°
	Φ	31.8°
Walk-off angle	**ρ**	0.0162 rad
Linear index of refr. at 798nm	n_o	1.611
Extr. index of refr. at 399nm	n_3	1.611

1.3.1.2 Third Harmonics Generation (THG)

Third Harmonics Generation (THG) is the coherent conversion of light with angular frequency ω into light with angular frequency 3ω, wavelength λ/3, in material that undergoes intensity irradiation. It includes the absorption of three identical photons of energy ($\hbar\omega$), ($\hbar=h/2\pi$) and the emission of a single photon of energy ($3\hbar\omega$), within the temporal uncertainty interval of ω^{-1}~10^{-16} s. The resultant light propagates in the forward direction [18].

A susceptibility tensor, $\chi^{(n)}$, describes the susceptibility of material to a given nonlinear conversion process, this susceptibility that relates to the polarization field *P*, induced in the material to the electric field *E*, of the incident photon .So from eq. (1.5) the third-order nonlinear susceptibility tensor $\chi^{(3)}_{ijkl}$, we are interested only in the terms associated with a uniformly polarized, single- angular frequency excitation field, i.e., $\omega_j=\omega_k=\omega_l$. This allows the third-rank tensor status of the susceptibility tensor to be suppressed and the THG polarization field $P^{(3)}(3\omega)$ to be expressed as:

$$P^{(3)}(3\omega) = \chi^{(3)}(3\omega)\, E^3(\omega) \ldots\ldots\ldots\ldots\ldots\ldots\ldots..\ldots\ldots\ldots(1.6)$$

$P^{(3)}(3\omega)$ is the third-order nonlinear polarization.

In a solution or other isotropic media, the measured value for $\chi^{(3)}(3\omega)$ is averaged over orientation and equal to :

$1/3\ \chi^{(3)}_{xxxx}(3\omega)+ \chi^{(3)}_{yyyy}(3\omega)+ \chi^{(3)}_{zzzz}(3\omega)$. [18]

Third harmonics were generated through two steps with second harmonics generation in a first crystal and sum frequency generation in a second crystal. [19]

Third Harmonics Generation (THG) is a nonlinear process, in which incident high intensity laser radiation at the angular frequency ω,

interacting with a nonlinear medium, causing to produce additional spectral component at the angular frequency 3ω. For a tight focused beam it can be generated only on the interface between two media.[20]

By one step the process of third harmonics generation could be produce in a single crystal. This means that only one optical component is required , which makes a very simple setup [9]. (see Fig. 1.4).
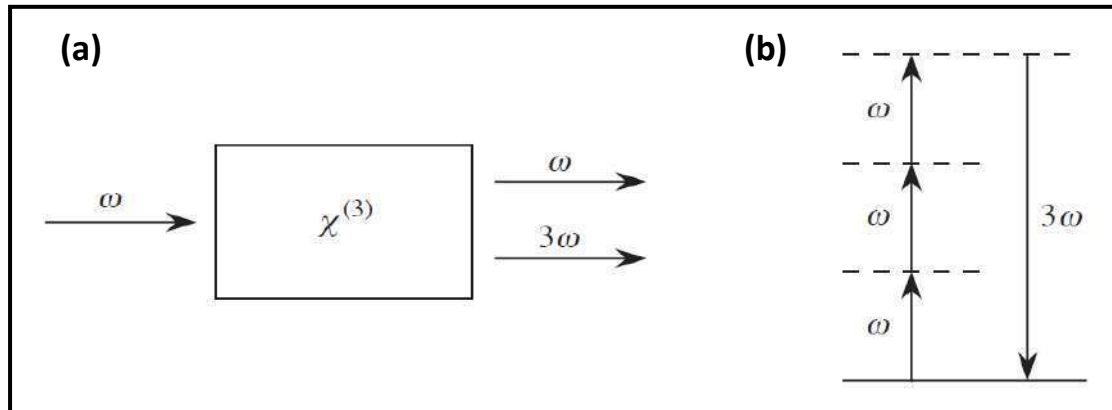
Figure (1.4) Third harmonics generation.

(a) Geometry of the interaction.(b) Energy-level description [15].

The real $(\text{Re } \chi^{(3)})$ and imaginary $(\text{Im } \chi^{(3)})$ parts of the third order nonlinear optical susceptibility $\chi^{(3)}$ were determined from experimental results of nonlinear refractive index n_2 and the nonlinear absorption coefficients β according to the following relations[21]:

$$\text{Re } \chi^{(3)}(esu) = 10^{-4} \frac{\varepsilon_0 C^2 n_o^2}{\pi} \left(\frac{cm^2}{W}\right) \quad \text{.................................(1.7)}$$

$$\text{Im } \chi^{(3)}(esu) = 10^{-2} \frac{\varepsilon_0 C^2 n_o^2 n_2 \lambda \beta}{4\pi^2} \left(\frac{cm^2}{W}\right) \quad \text{...............................(1.8)}$$

Where, c : is the speed of light, λ: is the wavelength.

The absolute value $\left|\chi^{(3)}\right|$ of was calculated from the following relation :

$$\left|\chi^{(3)}\right| = \left[(Re(\chi^{(3)}))^2 + (Im(\chi^{(3)})^2\right]^{\frac{1}{2}} \quad \text{.............................(1.9)}$$

1.3.1.3 High Harmonics Generation (HHG)

The generation of optical harmonics of very high order is one example of the many interesting new phenomena that occur when extremely intense ultrashort laser pulses interact with matter [22].

High harmonics generation (HHG) was discovered in 1987. Due to the progress in short pulse high energy Ti:sapphire lasers (30fs, 1mJ) it became possible to expose atoms to very high field strength before complete ionization and in 1997 electromagnetic Ultraviolet (EUV) radiation at wavelength 2.5 nm was obtained using HHG [23].

In high harmonics generation (HHG) the angular frequency of laser light is converted into its integer multiples. It can be easy that to generate Harmonics of high orders from atoms and molecules exposed to intense (usually near-infrared) laser fields. Amazingly, the spectrum from this process, generation of high harmonics, consists of a plateau where the harmonics intensity is nearly constant over many orders and a sharp cutoff (see Fig. 1.5) [24].
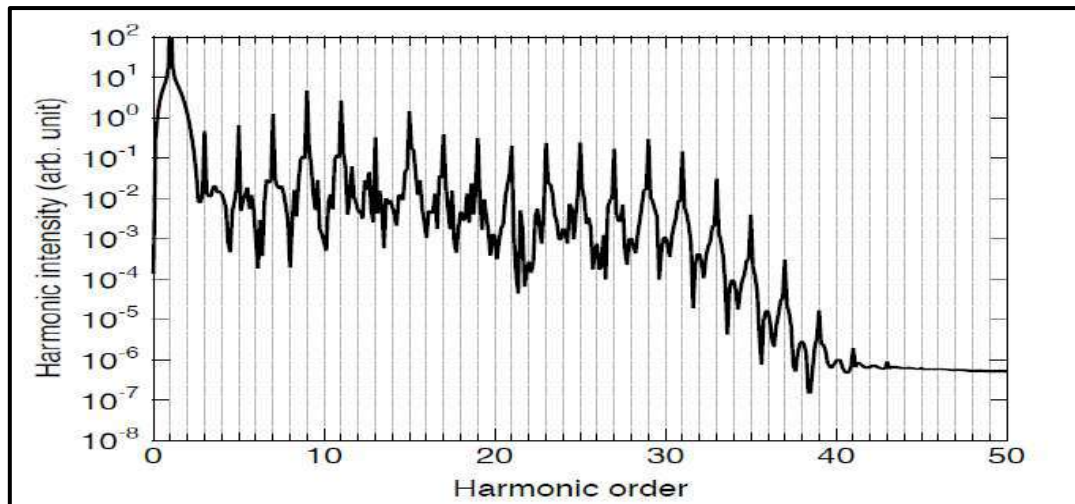
Fieger(1.5) HHG spectrum from a hydrogen atom, calculated with the

Eaceman-Rachford method [24].

This technique for producing short wavelength light was made possible by the development of ultrafast, high intensity laser sources. As with any

harmonics generation process, the main technical obstacle to a high conversion efficiency for HHG is the difference in the phase velocities between the fundamental and harmonics fields due to dispersion of the nonlinear material [25].

The higher order harmonics are generated at higher laser intensities. When the electric field strength of the laser is on the same scale as the inner atomic electric fields, it cannot be considered as a small perturbation anymore, i.e., perturbation theory breaks down [26].

1.3.2 Optical Parametric Oscillation

An Optical Parametric Oscillator (OPO) is a cavity containing a quadratic crystal[27]. Here laser power is applied to a non-linear crystal at a pump angular frequency ω_3. Energy (given in terms of the angular frequency $E = \hbar\omega$) and momentum (given in terms of the wavenumber $\mathbf{p} = \hbar k$) are preserved. Oscillations are caused in the crystal at frequencies ω_s and ω_i, the signal and idler frequencies respectively. The signal and idler frequencies are determined by the frequency condition.

$$\omega_p = \omega_s + \omega_i \ \dots\dots\dots\dots\dots\dots\dots\dots\dots\dots\dots\dots\dots\dots\dots\dots\dots(1.10)$$

and the phase matching condition

$$\Delta K = 0, \qquad K_3 = K_s + K_i \ \dots\dots\dots\dots\dots\dots\dots\dots\dots\dots\dots\dots\dots\dots.(1.11)$$

The two waves interact sufficiently when The phase matching occurs then will produce a calculable non-linear effects. Also the phase matching condition can be written as:

$$\omega_3 n_3 = \omega_1 n_1 + \omega_2 n_2 \ \dots\dots\dots\dots\dots\dots\dots\dots\dots\dots\dots\dots\dots\dots\dots(1.12)$$

where n_1 and n_2 are refractive index at angular frequencies ω_1 and ω_2 , they are determined by the propagation direction and polarization of the

modes at ω_1 and ω_2. In non-cubic materials, the refractive index depends on the direction of the E field relative to the crystallographic directions[28]. The special case we deal with is called Degenerate Parametric Down Conversion being $\omega_s = \omega_i \equiv \omega$ [27]

1.3.3 Frequency Conversion (FC):

The frequency conversion is a phenomena of two frequencies applied to a non-linear crystal to generate a sum frequency (up converter) or difference frequency (down converter), As shown in Fig.(1.6). These signals mix in the nonlinear medium to produce a signal [28], at $\omega_1 = \omega_3 - \omega_2$ (down converter), or at $\omega_1 = \omega_3 + \omega_2$ (up converter). Phase matching shows whether up-conversion or down-conversion actually occurs. From the signal of ω_3 the power drives the system at angular frequencies ω_1 and ω_2, and as a function of length of the nonlinear crystal, the amounts of power at ω_1 and ω_2 can be varied [28]. The up-conversion can be exploited to convert the signal of infrared in to the visible region when detectors are fast and sensitive so the frequency conversion is attractive for practical applications. Down-converters can be exploited to create a different angular frequency in the far infrared where high power sources have been unavailable until about 1965, when some far infrared lasers were first built [28].
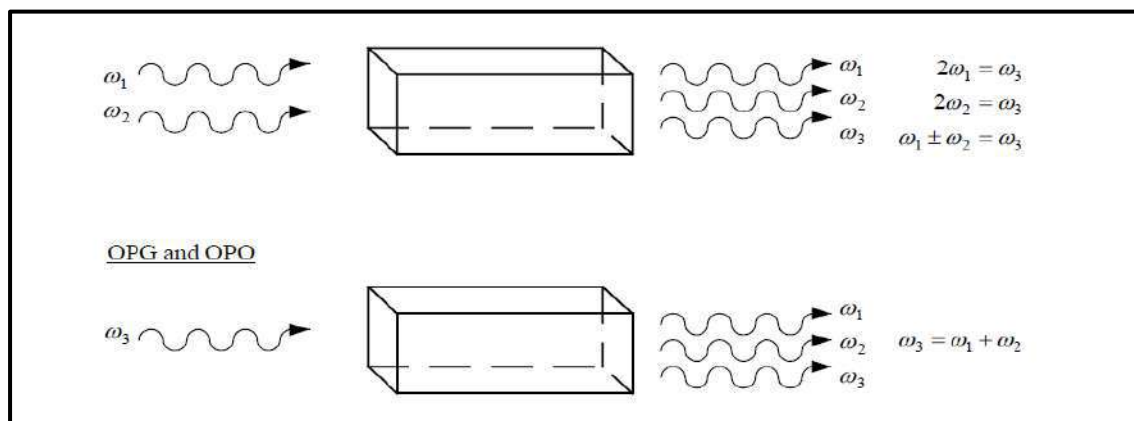
Figure (1.6) Frequency conversion processes arising from $\chi^{(2)}$ [29].

1.4 Phase Matching

Phase-matching is a technique which is borrowed from traditional nonlinear optics and here applied to extreme nonlinear optics [30]. In principle all the mixing processes in figure (1.6) will occur simultaneously when an acentric crystal is pumped by intensity laser beams, but most often only one process will grow strong over distance. The prevailing type will be the one for which the momentum of the photons that take part in the frequency conversion is conserved [29]. For angular frequency doubling it can be seen from equation (1.15) that the intensity at 2ω will oscillate back and forth when the wave is propagation through the material, if the phase-matching is not equal zero as it is seen in figure (1.7):

$$\Delta K = 2k_\omega - k_{2\omega} = \frac{2\omega(n_{2\omega} - n_\omega)}{c} \neq 0 \qquad ……..……..…………(1.13)$$

where, k_ω : is the wave-vector of the fundamental laser beam

$k_{2\omega}$: is the wave-vector of the second-harmonics laser beam [29]. The physical meaning behind eq.(1.13) is that the fronts of constant polarization for $P_{2\omega}$ moves with the phase velocity of the pump field i.e., c/n_ω, while on the other hand the generated wave $E_{2\omega}$, has the phase velocity $c/n_{2\omega}$ The driving polarization and the generated field will thus drift out of phase relative each other. After the distance L_c, the coherence length, the fields have accumulated a phase shift of π between each other and the energy will start to flow in the opposite direction instead, from the harmonics field back to the field at the fundamental angular frequency[30].
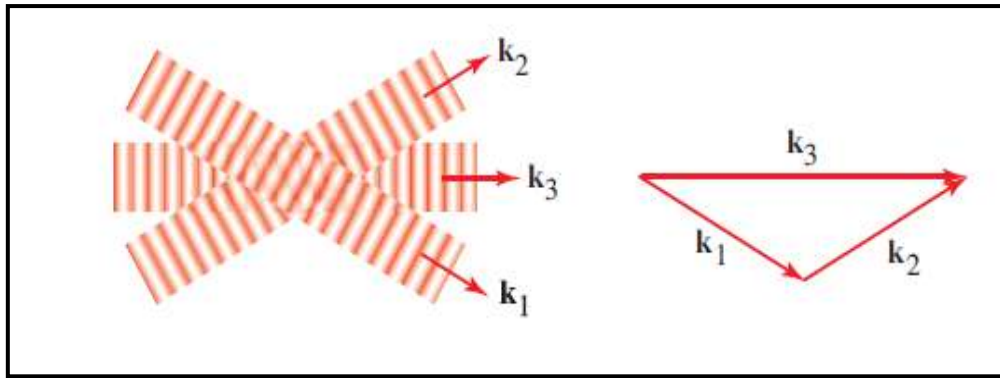
Figure (1.7) The phase matching condition[15].

Also in Fig.(1.8) the total output is sum, or the integration of the all dipoles at every position in the material. [31]
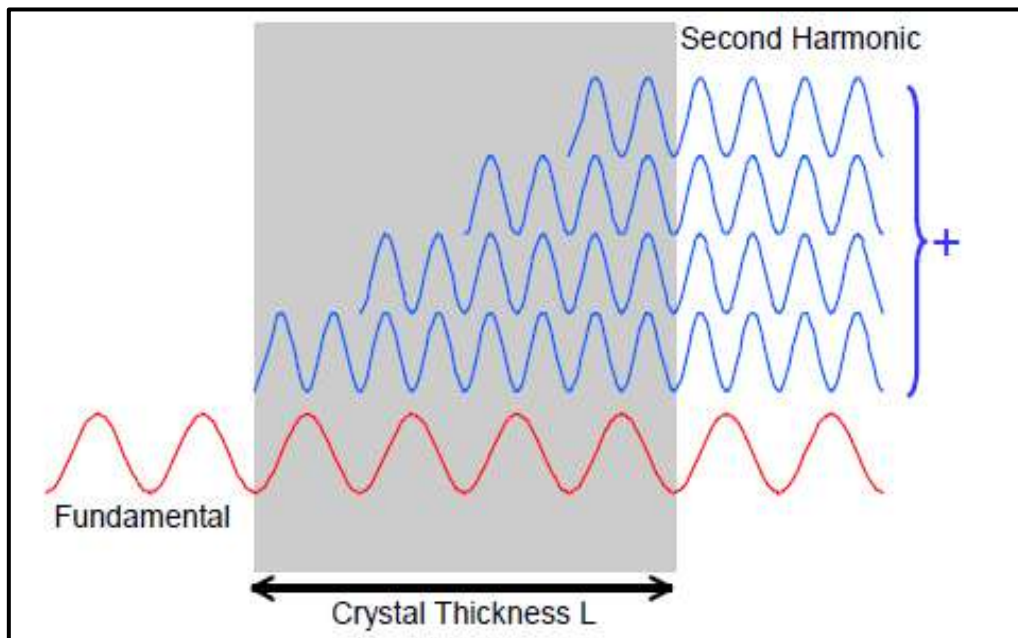
Fig(1.8) Concept of phase matching [31].

1.4.1 Phase Matching in High Harmonics Generation

Studying the HHG operation in a single crystal response basically provides the predicted shape of the harmonics spectrum. However, it cannot account for the observed harmonics yield. To obtain strong harmonics emission in a medium, propagation effects need to be considered. So far, there has been much work in which these problems have been investigated [26]. For coherent construction of the harmonics emission, the wave fronts of the fundamental laser and the generated

harmonics must be in phase. Atoms along the path of the laser produce harmonics propagating with the laser field. When they are in phase with the laser wave front, the distance over which the fundamental wave front and the harmonics wave front become out of phase is called the coherence length and is given by:

$L_c = \pi /\mathbf{\Delta k}$ …………………….…………………………..………(1.14)

where $\mathbf{\Delta k}$ is the phase mismatch.

For phase matching in the HHG process, one needs $\mathbf{\Delta k}_q = qk_\omega - k_q = 0$, where q is the harmonics order, k_q is the wave vector of the qth harmonics and k_ω is the wave vector of the fundamental beam.[26]

1.4.2 Quasi-phase matching (QPM)

Quasi-phase matching (QPM) is an alternative method for compensating the phase mismatch to improve conversion efficiency. In this technique, the phase of the driving laser is corrected at a periodicity equal to twice the coherence length, so that the destructive interference is eliminated. Several proposals and demonstrations of QPM of HHG have been published to date. However, many of these have technical limitations, or limited scaling to higher conversion efficiency. One of the reasons for this is that there has not been an easy, in-situ technique for measuring the dynamically changing coherence length of HHG [25].

1.5 Literature Survey

In the history of nonlinear optics, the discovery of optical harmonics generation marked the birth of the field . The effect has since found wide application as a means to extend coherent light sources to shorter wavelengths.

In 1989 Chen et al.[32], proved that the Lithium triborate crystal is considered as a technologically important material for diverse

applications, such as nonlinear optical materials, laser harmonics generation. It can produce not only relatively large second order susceptibility but also has a wide energy gap.

In 1991 A. Borsutzky et al.[33], presented a review of experimental data on the second and third harmonics generation of Nd:YAG laser radiation. The results demonstrate that in LBO crystal phase- matched sum-frequency mixing of UV and infrared laser light generates tunable radiation at wavelength as short as the transmission cut-off at wavelength 160nm.

In 1991 R. H. French et al. [34], studied the electronic structure of Lithium Triborate, coupled with experimental studies of the band gap, absorption edge, and valence bands, using vacuum ultraviolet spectroscopy and valence-band x-ray photoemission spectroscopy. The direct band gap of LiB_3O_5(LBO) was 7.78 eV, and the transparent wavelength was 159 nm.

In 1991 XIE Fali et al.[35], studied the efficient generation of deep Ultraviolet radiation at wavelength of less than 0.20 pm obtained, which shows that It could be produced high power radiation at 0.1914 pm via sum-frequency-mixing of two waves with wavelengths of 0.2128 and 1.9071 pm in LiB_3O_5 crystal. An average output power of about 2.0mW and a conversion efficiency of 8% have been achieved.

In 1993 G. C. Bahar et al.[36], Investigated the Nonlinear Ultraviolet Generation in LBO crystal by using Nd:YAG and a Nd:YAG-pumped dye laser to generate tunable deep ultraviolet radiation down to 240 nm in a Lithium Triborate crystal (LBO) by sum-frequency mixing. It was found that the longer wavelengths can be generated by a combination of harmonics generation of the dye laser and sum-frequency mixing.

In 1994 D. N. Nikogosyan [37], studied the optical and nonlinear optical properties of the lithium triborate (LiB_3O_5 or LBO) crystal and showed a description of its applications in nonlinear optics, he found that the transmission range was from 155 nm to 3200 nm and the linear absorption coefficient of LBO was 3.1×10^{-3} cm^{-1} in the spectral range (351-364) nm and 3.5×10^{-4} cm^{-1} at λ=1064 nm.

In 1999 I. N. Ogorodnikov et al.[38], studied the luminescence characteristics of crystalline lithium triborate LiB_3O_5 (LBO) and Investigate the excitation and photoluminescence spectra of nominally pure. The totality of the experimental data obtained permitted a conclusion that the LBO luminescence has an intrinsic nature and that it originates from radiative decay of relaxed electronic excitations.

In 2002 P.L. Ramazza et al.[39]. reported an experimental study of the generated the second harmonics in type I interaction in LBO crystal by using a Ti:Sa laser working in the picosecond administration at 786 nm , It was found that the second harmonics of red light is generated by means of type I interaction in the XY crystallographic plane of LBO samples cut at $\theta = 90^{\circ}, \phi = 33^{\circ}$.

In 2003 H.Q. Li et al.[40], reported on the optical parametric oscillator (OPO) using LBO crystal and pumped by 532 nm wavelength laser. It was found that the LBO crystal can be used as OPO nonlinear crystal to increase the conversion efficiency and raise the output power. With the available mirror set and satisfy LBO phase matching the wavelength converts from 778 to 1036 nm for signal wave as well as it will be increased the output power to 9.4 Watt at 900 nm.

In 2006 Burcu Ardiçoğlu et al.[41], checked in using the nonlinear optical (NLO) field devices and found that the using of new borate such as LBO crystal lead to an expanding the frequency range, that provided by using the sources of common laser.

In 2013 Abdulnabi H. Mohsin [42], designed and implemented an Ultraviolet laser have 355 nm wavelength then he used LBO nonlinear crystal for Sum Frequency Generation (SFG) to obtain third harmonics generation (THG). It was found that the maximum third harmonics conversion efficiency due to SFG stage was 6.1%.

1.6 Aim of the Present work

The design of an optical system working to study:

 1. The optical linear and nonlinear properties for LBO, the linear deals with the refractive index, linear Absorption coefficient, the extinction coefficient, reflectance, optical conductivity and dielectric constant(ε). While the nonlinear optical properties could be represented by nonlinear refractive index and absorption coefficient for different wavelengths and output powers.
 2. The study also discusses the possibility of generating the higher harmonics in Lithium Triborate crystal.

CHAPTER TWO

THEORETICAL PART

2.1 Introduction

The theoretical consideration, considered in this chapter, includes the solid crystal concepts and the relation between these concepts and the nonlinear media, which is represented in this work by refined lithium triborate crystal .A crystal study carried out on the effective of nonlinear optical properties of the medium and its applications. It explains the third dimension scanning technology(Z-Scan).

2.2 Lithium Triborate Crystal

The existence of Lithium Triborate (LiB_3O_5) was already found in 1926 by Mazetti and Carli . However, it took until 1989 that the excellent nonlinear properties of LBO crystal was discovered [43].

The LBO crystal is a negative biaxial crystal, it belongs to the point group mm2. The crystal structure is based on a large number of anionic boron-oxygen bonds $(B_3O_7)^{5-}$ organized around Lithium (Li^+) cations. It is the anionic group, which is assumed to be responsible for the basic nonlinear properties of Borate crystals as LBO or others like BBO. LBO crystal have wide applications in nonlinear optics, because of LBO crystal's high optical damage threshold (for damage in the crystal bulk) and being highly transparent from the near Infrared to the near Ultraviolet [44].
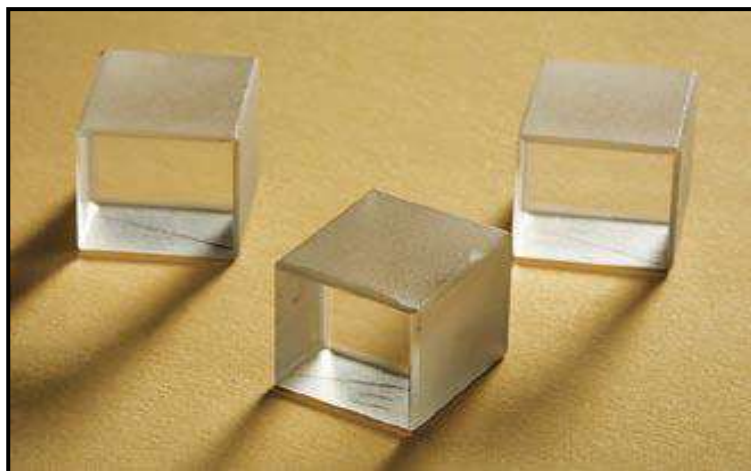
Figure (2.1) Lithium Triborate crystal [45].

LBO single crystal is considered to be one of the most popular nonlinear optical crystals especially for frequency conversion [46], as a result of its excellent optical properties , such as :

1. The second-order nonlinear optical coefficient of is large (d_{eff} = 50.96 pm/V).

2. The laser damage threshold is higher about ($45GW/cm^2$ at wavelength 1.064μm, 1ns pulse) makes LBO single crystal very suitable for harmonics generation of high intensity laser radiation in a wide spectra.

3. Broad transparency range (0.16 - 2.6) μm, and good chemical and mechanical stability.

4. The physical properties, such as infrared reflectance, Raman spectra, elastic properties and dielectric properties, as well as its optical properties[47]. This Physical and chemical Properties of LBO crystal are listed in table (2.1).

Table (2.1) LBO Crystal Structural, Physical and chemical Properties[48].

Chemical Formula	LiB_3O_5
Crystal Structure	Orthorhombic, Space group $Pna2_1$, Point group mm2
Lattice Parameter	a=8.4773Å, b=7.3788Å, c=5.1395Å
Melting Point	834°C
Mohs Hardness	6
Density	2.47 gm/cm^3
Absorption coefficient	< 0.1%/cm at 1064nm < 0.3%/cm at 532nm
Specific heat	1.91J/cm^3.K, 1060 J/kg.K
Hygroscopic susceptibility	Low
Damage threshold	25 J/cm^2 (1064 nm, 10ns pulses)
Thermal Conductivity	3.5W/m/K
Thermal Expansion Coefficient	α_x=10.8x10^{-5}/K, α_y= -8.8x10^{-5}/K, α_z=3.4x10^{-5}/K

2.2.1 Some Optical Properties Of Lithium Triborate

LiB_3O_5 single crystal is orthorhombic with four formulae units per unit cell. The space group of LBO crystal is $Pna2_1$ (C_{2v}^9), while the point group is mm2, and the lattice parameters are a=8.4773 Å, b=7.3788 Å, and c=5.1395 Å[48]. The structural unit of Lithium Triborate (LiB_3O_5) consisted of the anionic group $(B_3O_7)^{5-}$ with one BO_4 tetrahedron and two BO_3 trigonal [49]. Figure (2.2) shows a projection of the LiB_3O_5 structure onto the (010) and the(001) planes. The boron atoms are located within coordination polyhedra of two types, triangles [B(1) and B(2)] and tetrahedra [B(3)]. The B(1) and B(2) atoms lie within planar triangles formed by oxygen, and the B(3) atoms within oxygen tetrahedra. The average nearest neighbor distance of B(1)-O is 1.3692 Å, of B(2)-O is 1.3713 Å, and of B(3)-O is 1.473 Å. There are four Li atoms in a cell, and they are associated with four oxygen atoms in a considerably distorted tetrahedron. The Li–O distance is rather longer than the B–O distance and ranges from 1.9887 to 2.1722 Å with a distorted tetrahedral coordination[50].

• : Li   **○ : O**   **⊘ : B**

(a) (010) projection   **(b) (001) projection**
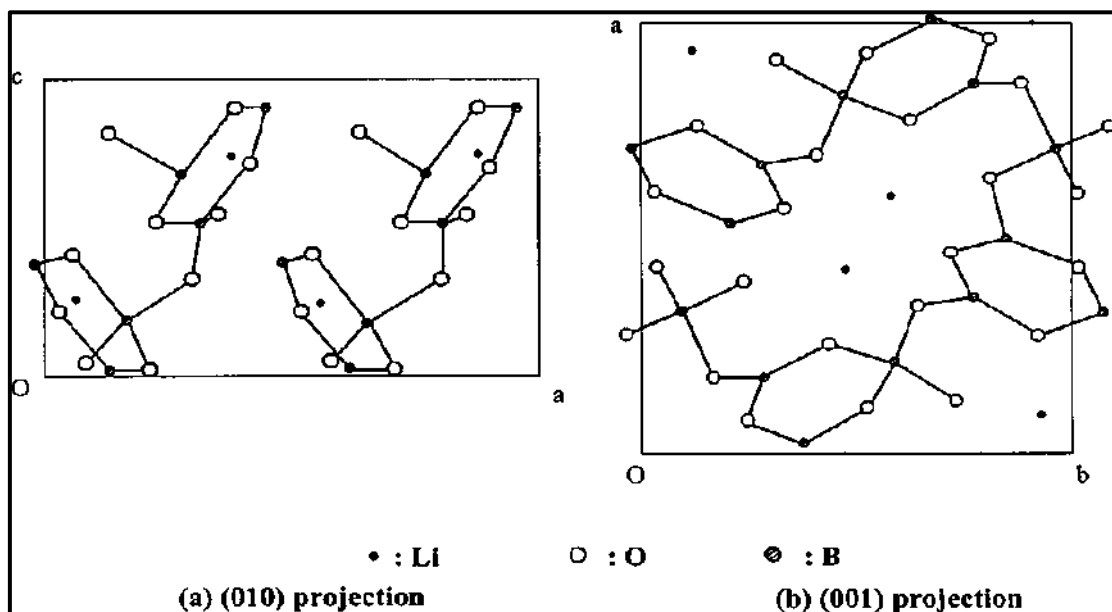
Figure (2.2) Projection of the crystal structure of a LiB_3O_5 single crystal[46].

2.2.1.1 The Transmission Property of LBO

LBO crystal have a wide range of transparency between (0.16-2.6)μm as shown in figure (2.3). This feature of LBO is ahead of other borate crystals for large transparency at the practical wavelength, LBO crystal have much higher pulse energy and high average power of the Nd:YAG laser because of the Nd:YAG laser damage threshold was about 40 GW/cm^2 [48].
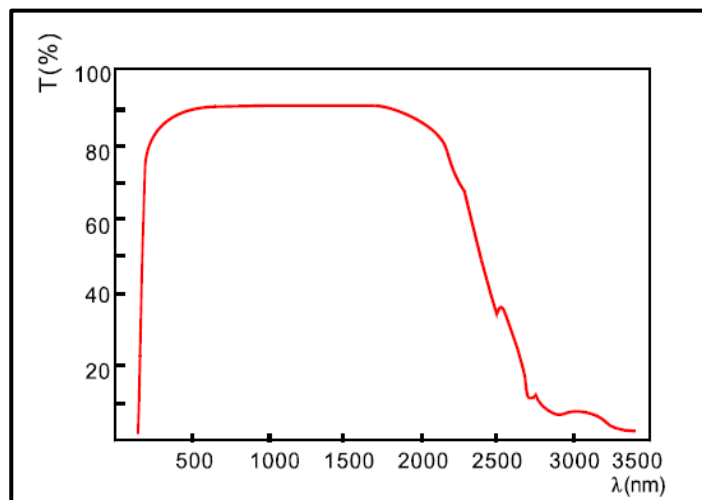
Figure (2.3) Transparency curve of LBO[51].

2.2.1.2 SHG and THG at Room Temperature

LBO is phase matchable for the SHG and THG of Nd:YAG laser, using either type I and type II interaction. For the SHG at room temperature, type I phase matching can be reached and has the maximum effective SHG coefficient in the principal XY and XZ planes (as it is seen in Fig. 2.4) [52], in a wide wavelength range from (551- 2600) nm (the effective SHG coefficient see Table 2.2). The optimum type II phase matching falls in the principal YZ and XZ planes (see Fig.(2.4)- the effective SHG coefficient see Table (2.2)). SHG conversion efficiencies more than 70% for pulsed and 30% for CW Nd:YAG laser, and THG conversion efficiency over 60% for pulsed Nd:YAG laser have been

observed[52].
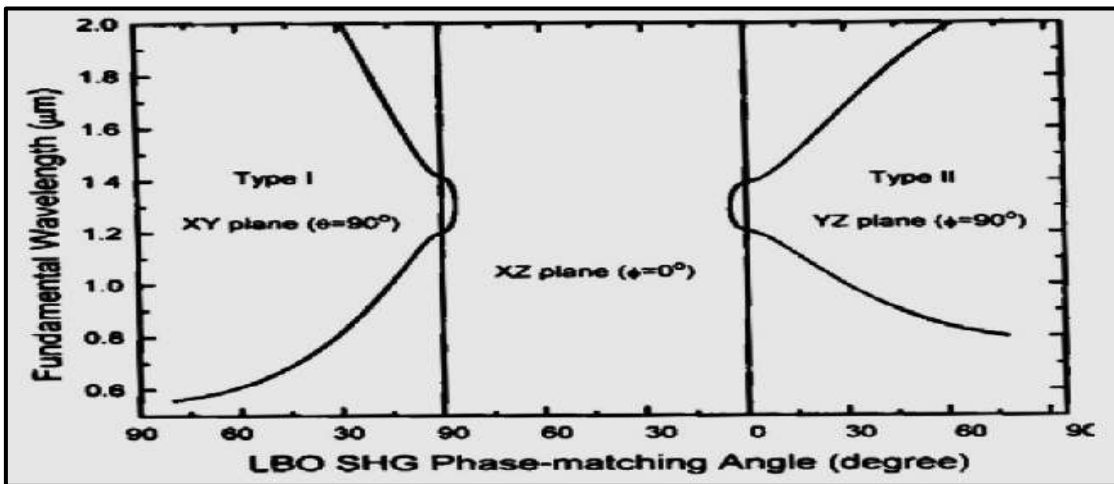
Figure(2.4) SHG tuning curves of LBO crystal [52].

Table (2.2) Linear and Nonlinear Optical Properties of LBO crystal[47]:

Linear Optical Properties	
Refractive indices: **at 1064 nm** **at 532 nm** **at 355 nm**	$n_x = 1.5656,\ n_y = 1.5905,\ n_z = 1.6055$ $n_e = 1.5785,\ n_o = 1.6065,\ n_z = 1.6212$ $n_e = 1.5971,\ n_o = 1.6275,\ n_z = 1.6430$
Therm-optic Coefficient **(/ °C , λ in μm)**	$dn_x/dT = -9.3 \times 10^{-6}$ $dn_y/dT = -13.6 \times 10^{-6}$ $dn_z/dT = (-6.3 - 2.1\lambda) \times 10^{-6}$
Sellmeier Equations **(λ in μm)**	$n_x^2 = 2.454140 + 0.011249/(\lambda^2 - 0.011350) - 0.014591\lambda^2 - 6.60 \times 10^{-5}\lambda^4$ $n_y^2 = 2.539070 + 0.012711/(\lambda^2 - 0.012523) - 0.018540\lambda^2 + 2.00 \times 10^{-5}\lambda^4$ $n_z^2 = 2.586179 + 0.013099/(\lambda^2 - 0.011893) - 0.017968\lambda^2 - 2.26 \times 10^{-5}\lambda^4$
Nonlinear Optical Properties	
SHG Phase Matchable Range	**551-2600nm (Type I) 790-2150 nm (Type II)**
Acceptance Angles **(@1064nm)**	**6.54mrad·cm (ϕ, Type I, SHG)** **15.27mrad·cm (θ, Type II, SHG)**
Temperature Acceptance	**4.7°C·cm(Type I, 1064 SHG)** **7.5°C·cm(Type II,1064 SHG)**
Spectral Acceptance	**1.0nm·cm (Type I, 1064 SHG)** **1.3nm·cm (Type II,1064 SHG)**
Walk-off Angles **(@1064 nm)**	**0.60°(Type I SHG)** **0.12°(Type II SHG)**
NLO Coefficients	$d_{eff}(I) = d_{32}\cos\varphi$ (Type I in XY plane) $d_{eff}(I) = d_{31}\cos^2\theta + d_{32}\sin^2\theta$ (Type I in XZ plane) $d_{eff}(II) = d_{31}\cos\theta$ (Type II in YZ plane) $d_{eff}(II) = d_{31}\cos^2\theta + d_{32}\sin^2\theta$ (Type II in XZ plane)
Non-vanished NLO susceptibilities	$d_{31} = 1.05 \pm 0.09$ pm/V $d_{32} = -0.98 \pm 0.09$ pm/V $d_{33} = 0.05 \pm 0.006$ pm/V
Electro-optic coefficients	$\gamma\,11 = 2.7$ pm/V, $\gamma\,22, \gamma31 < 0.1\gamma11$
Conversion Efficiency	**>90% (1064 -> 532nm) Type I SHG**
Damage threshold **at 1064nm** **at 532nm** **at 355nm**	**45 GW/cm^2 (1 ns); 10 GW/cm^2 (1.3 ns)** **26 GW/cm^2 (1 ns); 7 GW/cm^2 (250 ps)** **22 GW/cm^2**

2.2.1.3 Noncritical Phase Matching

The noncritical phase-matching (NCPM) means that all parts still fixed during scanning (no rotating parts). While the beam pointing is defined by the flat output coupler, it is independent of the signal wavelength and no adjustments are required in the coherent anti-Stokes Raman Scattering (CARS) setup. Only the OPO cavity length has to be adjusted for the variation in round-trip time [53]. It can be observed in the table (2.3), that the Non-Critical Phase-Matching (NCPM) of LBO is distinguished by no walk-off, wide acceptance angle and maximum effective coefficient. SHG conversion efficiencies of more than 70% for pulse and 30% for CW Nd:YAG lasers have been obtained, with good output stability and beam quality [52].

Table (2.3) Properties of type 1 NCPM SHG at 1064 nm [52]

NCPM Temperature	148°C
Acceptance Angle	52 mrad-cm$^{1/2}$
Walk-off Angle	0
Temperature Bandwidth	4°C-cm
Effective SHG Coefficient	2.69 d_{36}(KDP)

As it is shown below in Fig.(2.5), type I and type II Non-Critical Phase-Matching can be reached along x-axis and z-axis at room temperature, respectively.
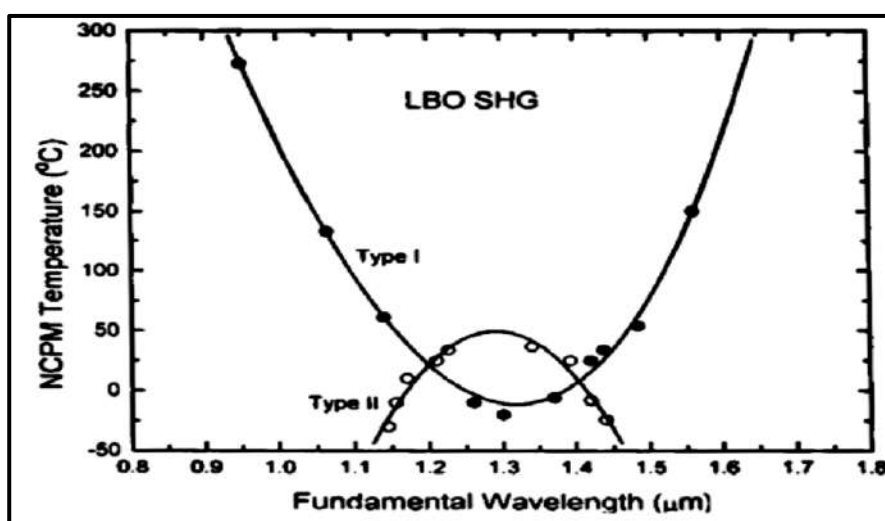
Figure (2.5) NCPM temperature tuning curves of LBO[54]

2.3 Z-Scan Technique

In 1990 M. Sheik-Baha, established a measurement method with the purpose of determining the nonlinear refraction of thin samples. This is called the Z-scan technique [55,56]. It is a single-beam technique that gives us both the sign and magnitude of refractive index nonlinearities and nonlinear absorption, which are associated with the real part $\chi_R^{(3)}$ and imaginary part $\chi_I^{(3)}$ of the third order nonlinear susceptibilities[57]. The Z-Scan technique has been used to measure the nonlinear optical properties of semiconductors, dielectrics, organic or carbon-based molecules and liquid crystals [58].

This method is rapid, simple to perform and accurate, therefore, it is often used. It is especially adequate for determination of a nonlinear coefficient for a particular wavelength. The essential geometry is shown in Figure (2.6) [59].
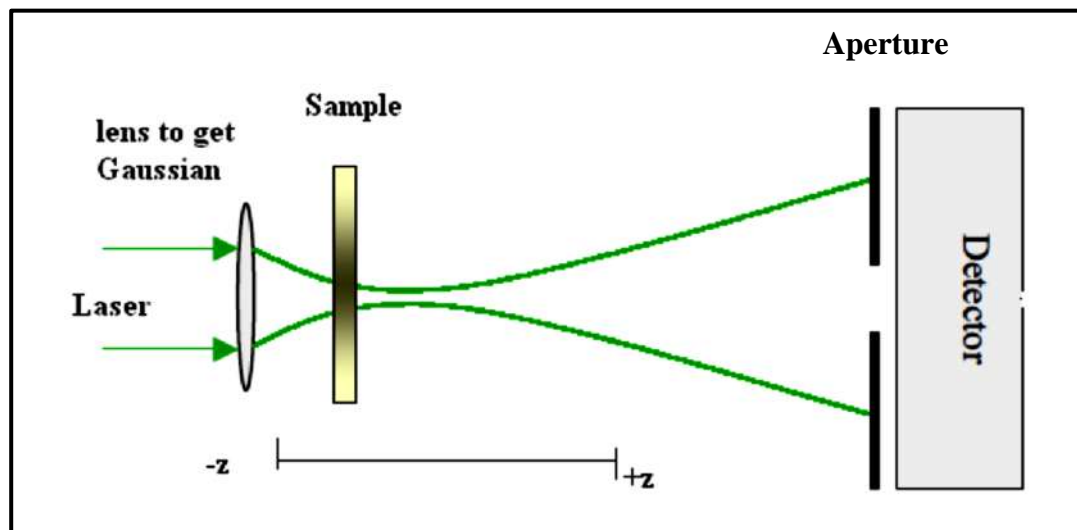
Figure (2.6) Z-Scan experimental arrangement [59].

The Z-Scan technique includes that the sample is scanned along the Z direction through the beam waist of a focused Gaussian laser beam in a tight focusing configuration, as in figure (2.6). As the sample approaches

focus the spot size decreases, increasing the irradiance on the sample and the induced nonlinear effects [60].

The original method suggested the use of a single beam incident on the sample. While, in principle, the method is simple, in practice, since lasers possess intensity fluctuations and the detector measures intensity loss due to both linear and nonlinear processes [61].

2.3.1 Types of Z- Scan Technique

There were two kinds of the Z-scan technique : closed aperture and open aperture. The advantage of using closed aperture is to measure the sign and magnitude of both nonlinear refractive index, the real and imaginary part of susceptibility, this susceptibility depends on the intensity pump of laser and on the absorption cross section at the excitation wavelength. The second part of Z-Scan technique is open aperture, this technique helps to calculate the nonlinear absorption coefficient β [62].

2.3.1.1 Closed Aperture Z-Scan :

In the closed aperture Z-scan technique [figure (2.7)] an aperture should restrict some undesired outside scattered light from reaching the detector. A lens focuses a laser beam to a waist point, and after this point the beam is defocused. Afterwards an aperture is placed with a detector behind it. The aperture favors such geometry that only the light the central region of cone can reach the detector [63]. This method considered to be one of the most important and useful mothed to calculate the magnitude and sign of the nonlinear refractive index from the transmission curve. If the nonlinear refractive index n_2 of the sample is negative, the beam gets converged in the pre-focal region to get focused closer to the aperture. Consequently, the beam diameter decreases near the aperture, resulting in large amount of through put at the detector [64]. Material with a negative

nonlinear refractive index and thickness smaller than diffraction length of the focused beam, is regarded as a thin lens of variable focal length. Starting the scan the sample is moved from a distance far away from the focus close to the lens (negative Z direction) the beam irradiance on the sample is low and negligible nonlinear refraction resulting in relatively constant transmittance, this results of a peak in the pre focal region [65]. While in the post focal region, the same phenomenon results in the divergence of the beam, which results in the decreased transmission through the aperture. Hence, a valley appears in the post-focal region. If the sample has positive nonlinear refractive index, it has just the opposite result (pre focal valley and post focal peak.), the first is called self-defocusing, while the second is called self-focusing [64].
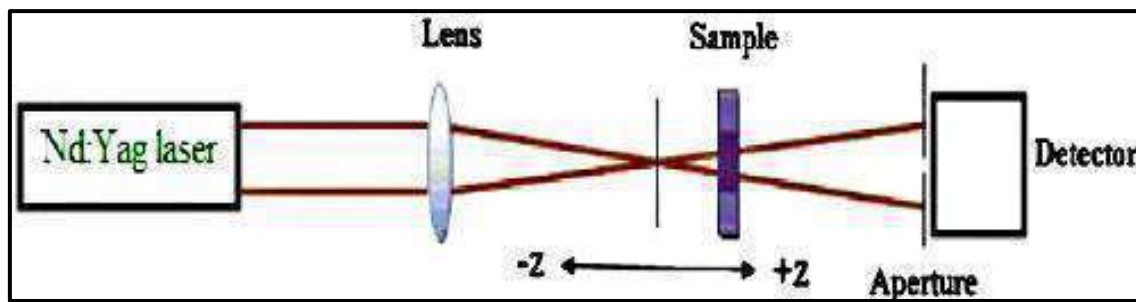
Figure (2.7) : Illustration of the experimental setup for closed Z-Scan [61].

We use a Gaussian laser beam and then the transmittance of the beam through the experimental system is measured. We have to change a position of the sample with respect to the focal plane of a field lens, which is set at position z = 0 [57].

Figure (2.8) showed that the measurement starts far away from the focus (negative z), where the transmittance is relatively constant (figure 2.8 a). Then the crystal is moved towards the focus and then to the positive z (figure 2.8 b to h). If the material has a positive nonlinearity ($n_2 > 0$), the T(z) graph has a valley first and then a peak. For the crystal with ($n_2 < 0$) the graph is exactly the opposite (first the peak and then the valley) [57].
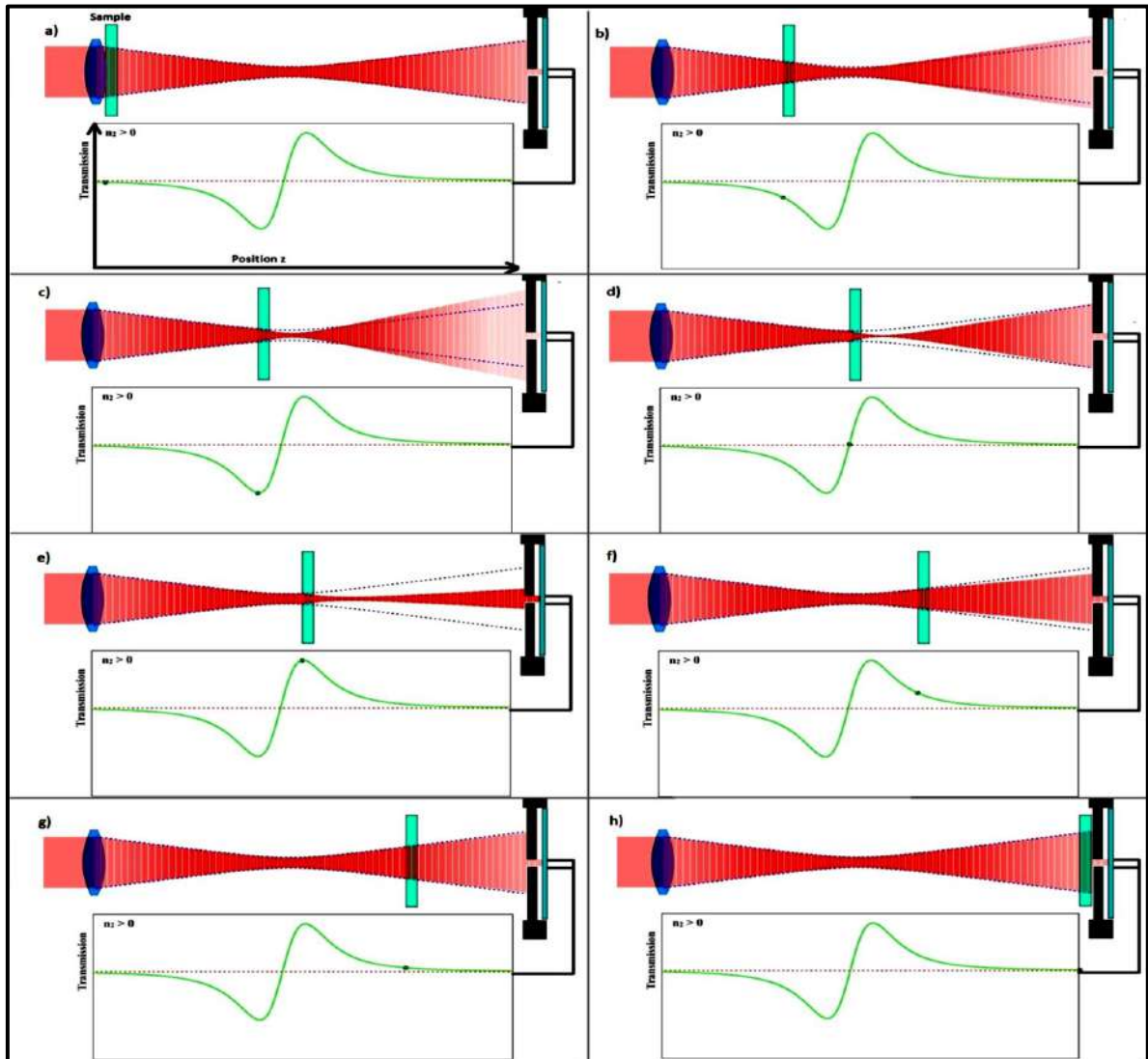
Figure (2.8) The Z-scan measurement as represented in an online animation, we can see the change of the laser beam and the change of the transmittance at the same time [57].

While figure (2.9) showed the order of scanning the third dimension of positive and negative nonlinear refractive index.
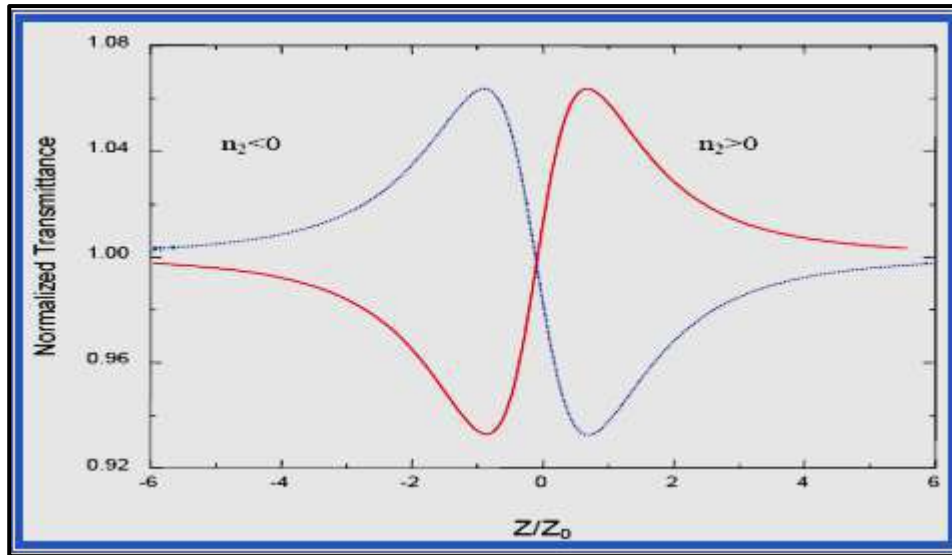
Figure (2.9) Z-Scan technique closed– aperture Order curves of positive and negative nonlinear refractive index [57].

By observation the transmittance change through a small circular aperture placed at the far-field position, one able to determine the nonlinear refractive index. The crystal was moved in step of 1 mm during the scan[57].

The relation between the normalized transmittance T(z) and z position was obtained by moving the crystal along the axis of the incident beam (z-direction) with respect to the focal point. We define an easily measurable quantit, $\Delta T_{p-v} = T_p - T_v$ as the difference between the normalized peak and valley transmittance. Analysis shows that variation of ΔT_{p-v} is linearly-dependent on the temporally averaged induced phase distortion, defined here as $\Delta\Phi_o$. If the Z-scan aperture is closed to allow linear transmission of less than 10 percent, and ΔT_{p-v} <1 The variation of this quantity as a function of $\Delta\Phi_o$ is given by [66]:

$$\Delta T_{p-v} = 0.406 \, |\Delta\Phi_o| \dots\dots\dots\dots\dots\dots\dots\dots\dots\dots\dots\dots\dots\dots\dots(2.1)$$

Where, 0.406 is constant quantity.

The non-linear refractive index (n_2) can be obtained from the formula [67]:

$$n_2 = \Delta\Phi_o / I_o L_{eff} k \quad ....(2.2)$$

Where,

I_o: is the laser beam intensity at the focus (Z = 0), k : the wave number,

L_{eff}: is the effective thickness of the crystal.

$$k = 2\pi/\lambda \quad ....(2.3)$$

Where, λ: is the wavelength of the laser beam.

$$I_o = 2 \, \wp /\pi w_o{}^2 ....(2.4)$$

Where, $\wp$: power of laser beam, w_o: the beam radius at the focal point

$$L_{eff} = (1 - \exp(-\alpha_o t))/\alpha_o \quad ....(2.5)$$

t: is the thickness of the crystal, the linear absorption coefficient α_o, which can be found from the curved transmission [68].

$$\alpha_o = \frac{1}{t} Ln \frac{1}{T} \quad ....(2.6)$$

Where T: the transmittance .

2.3.1.2 Open Aperture Z-Scan:

The nonlinear absorption coefficient β of LBO crystal is manifested in the open aperture Z-Scan measurements. For example, if nonlinear absorption like two-photon absorption (TPA) is present, it is manifested in the measurements as a transmission minimum at the focal point. On the other hand, if the crystal is a saturable absorber, transmission increases with increase in incident intensity and results in a transmission maximum at the focal region. It has been shown that the model originally developed by Bahae et. al. for pure (TPA) can be also applied to excited state absorption [64]. In this technique the aperture placed close to the detector which is removed and the crystal transmission for different position (Z) values is measured as before as shown in Fig.(2.10).
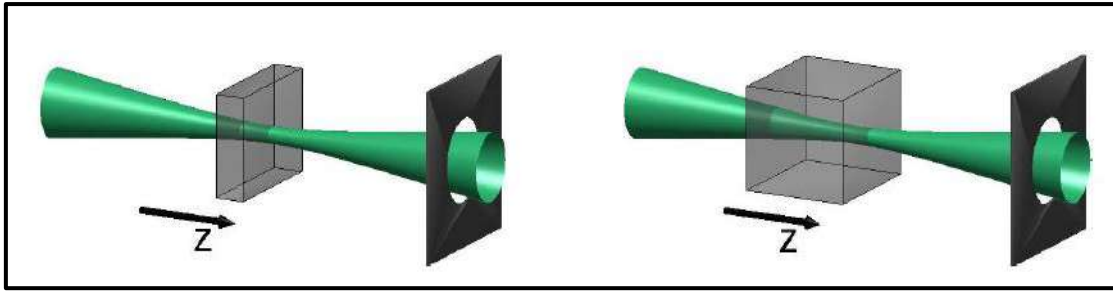
Figure (2.10) : The technique of Z-Scan: open aperture, the integrated light
   intensity is measured as a function of crystal position. Left: thin sample
   ($< z_o$ Rayleigh length), right: thick sample ($> z_o$ Rayleigh length) [69].

In Fact, the nonlinear absorption coefficient β can be easily calculated
from the transmittance curves figure (2.11) [59]:

$$\beta = \frac{2\sqrt{2}}{I_0 \, L_{eff}} \Delta T \dots\dots\dots\dots\dots\dots\dots\dots\dots\dots\dots\dots\dots\dots\dots\dots\dots\dots\dots\dots\dots\dots..\dots(2.7)$$

Where ΔT is the one peak or one valley value at the open aperture Z-scan
curve.

Figure (2.11) shows forms of Z-Scan technique open aperture,
   a. Two photon absorption, b. Saturated absorption [70].

2.4 Linear Optical Properties

The refractive index is an important parameter for optical materials and applications. Thus, it is important to determine optical constants of the crystal. The refractive index of the crystal can be easily calculated from the reflectance values [71]:

$$n = [\frac{4R-K^2}{(R-1)^2}]^{0.5} - \frac{R+1}{R-1} \dots\dots\dots\dots\dots\dots\dots\dots\dots\dots\dots\dots\dots\dots(2.8)$$

Where R is the reflectance and K is the extinction coefficient.

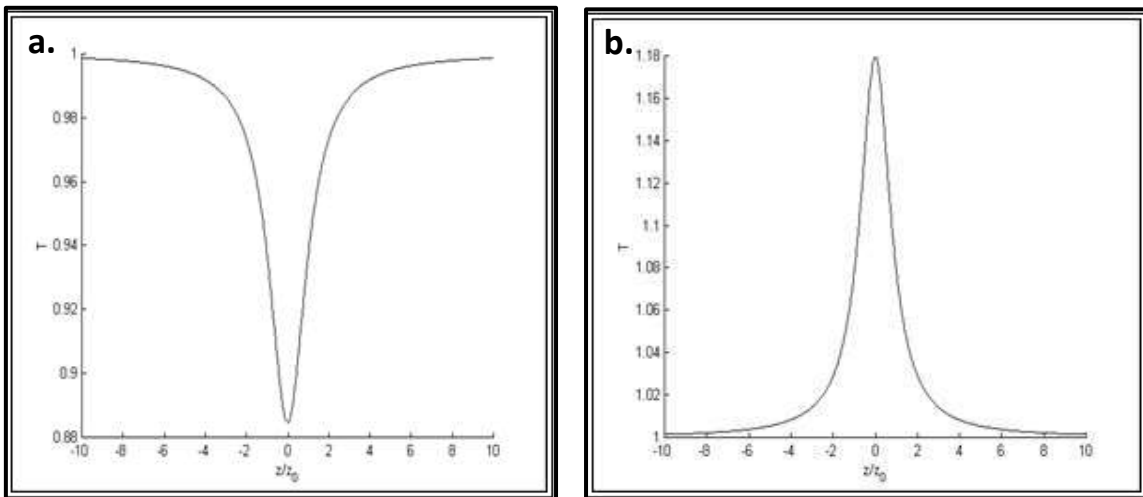The reflectance value (R) was calculated by using the equation (2.9) below;

$$R= 1- (A+T) \dots\dots\dots\dots\dots\dots\dots\dots\dots\dots\dots\dots\dots\dots\dots\dots..(2.9)$$

Where A is the absorbance.

The extinction coefficient can be calculated from the absorption coefficient:

$$K = \alpha\lambda/4\pi \dots\dots\dots\dots\dots\dots\dots\dots\dots\dots\dots\dots\dots\dots\dots\dots\dots.(2.10)$$

where (λ) is the wavelength of the incident radiation and (α) the absorption coefficient.

The absorption coefficient (α) is computed using the above equation at any given wavelength.

The optical conductivity σ is related to the absorption coefficient α by[72]:

$$\sigma = \alpha nc/4\pi \dots\dots\dots\dots\dots\dots\dots\dots\dots\dots\dots\dots\dots\dots\dots\dots.(2.11)$$

Where c is the speed of light. The optical conductivity (σ) can easily be computed if (α) and (n) are known.

The complex dielectric constant (ε) is given by [71]:

$$\varepsilon= (\varepsilon_1 - i\varepsilon_2) \dots\dots\dots\dots\dots\dots\dots\dots\dots\dots\dots\dots\dots\dots\dots\dots(2.12)$$

So, the real and imaginary parts of the dielectric constant are related to the n and K values from which arise [72]:

$$\varepsilon_1 = n^2 - K^2 \dots\dots\dots\dots\dots\dots\dots\dots\dots\dots\dots\dots\dots\dots\dots..\dots..(2.13)$$

$\varepsilon_2 = 2nK$ …………………………………………………………..(2.14)

2.5 The conversion efficiency of Harmonics Generation :

At every position in the crystal, the non-linear polarization creates a dipole emitter that radiates at twice the fundamental frequency. At every time the relative phase of these dipoles is given by the non-linear polarization generated by the fundamental wave, that gives the conversion efficiency of second-harmonic generation [31]:

$\eta_{SHG} = I(2\omega)/I(\omega)$…………………………………………..…..(2.15)

Therefore proportional to L^2 [31]:

$$\eta_{SHG} = (\frac{\sin(\Delta KL/2)}{(\Delta KL/2)})^2 \text{…………..…………………………………....(2.16)}$$

Where, ΔK which described in Eq.(1.20) This sinc function has a maximum for $\Delta K = 0$ where $\eta = 1$.

For third harmonics generation, the intensity is related to the path length of the beam inside of the nonlinear medium, and can be described by [73]:

$$I_{3\omega} = \frac{(3\omega)^2}{n_\omega^4 c^4 \varepsilon_0^2} \times \frac{\sin^2[(\frac{\Delta KL}{2})]}{(\Delta KL/2)} |\chi^{(3)}|^2 L^2 I_\omega^2 \text{ …………………………….(2.17)}$$

Where,

$\Delta K = k_{3\omega} - 3k_\omega$, $I_{3\omega}$: the intensity of third harmonics generation beam, I_ω: the intensity of the input beam at frequency ω, L: crystal length.

Therefore, the efficiency of the conversion of a fundamental into third harmonics generation can be approximated as [19]:

$$\Omega_3 = \frac{\omega^2}{n_{3\omega} n_\omega^3 \varepsilon_0^2 c^4} |\chi^{(3)}|^2 I_\omega L_{eff}^2 \text{ ………..………………….....(2.18)}$$

Where,

L_{eff}. the effective length, which described in Eq. (2.5) previously.

CHAPTER THREE

EXPERIMENTAL PART

3.1 Introduction

This chapter includes the materials, devices that are chosen to be used for the present work and it explain the Z-Scan technique to measure the nonlinear optical properties. The measurements were done at wavelengths (532 nm and 1064 nm) respectively.

3.2 Spectrophotometer

Spectrophotometer was used to measure the transmission and absorption spectra of LBO crystal as is it seen in figure (3.1), while the properties of the UV-Visible Spectrophotometer are listed in Table (3.1).

Table (3.1) Properties of the UV-Visible Spectrophotometer

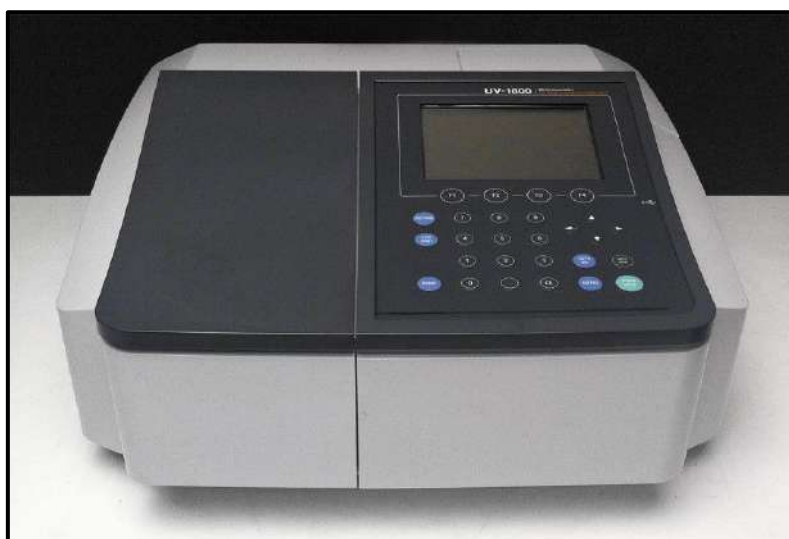| Wavelength rang	190-1100 nm
Light source	6V 10W Tungsten halogen lamp
Wavelength scan rate	Maximum 1000 nm/min
Power requirements	220-240 V .AC
Detector	Silicon photodiode

Figure (3.1) UV-Visible spectrophotometer

3.3 The Z –Scan system

Z-Scan measurements were performed in two parts, closed and open aperture, with two input energies. Each case was employed in two wavelengths 532 nm and 1064 nm respectively. The closed-aperture Z-Scan was used to measure the nonlinear refractive index, while the open-aperture Z-Scan was used to measure the nonlinear absorption coefficient. In each wavelengths Z-Scan experiment were performed with two directions (transmission and reflection). Figure (3.2) shows the set-up of the Z-Scan system.

Mirror   Detector   Pinhole   He:Ne laser   Crystal   Lens   Nd:YAG laser
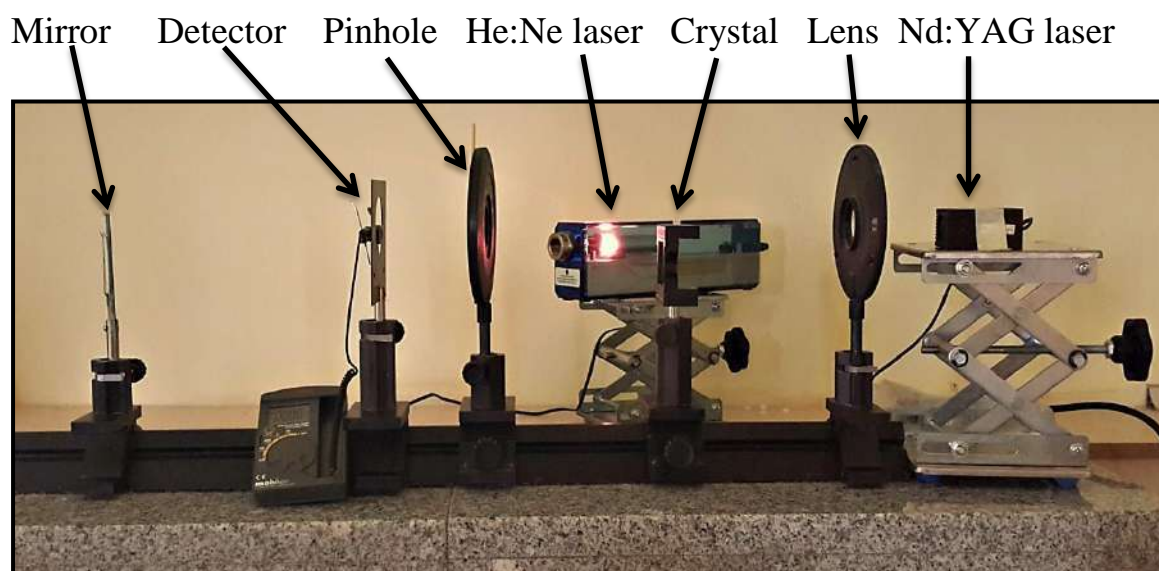
Figure (3.2)The set-up of Z-Scan technique

3.3.1 The Optical Elements Of Z-Scan Technique

The He:Ne laser was used for alignment of the optical set-up. The He:Ne laser was placed perpendicular to the setup. Then, the mirror reflected the laser beam inside the setup. The second element of Z-Scan system is a collimating lens whose focal length is 15 cm, the lens was placed opposite the Nd:YAG laser. The plane mirror was used in alignment, which reflects the laser beam of He:Ne laser backward, and

partially transmits laser beam toward Nd:YAG laser source. The third optical element is the pin hole, which is placed between the crystal and nearest to the detector. The diameter of pin hole is 1mm. The fourth optical element in Z-Scan system is the optical thermal detector, which is used to measure the output power of CW laser. The detector was placed at the far field of a Gaussian laser beam when the He:Ne laser is removed after alignment.

3.3.1.1 Nd:YAG Laser

This work has been done using Nd : YAG laser. At wavelength 532 nm in two powers (25 and 40 mW) and 1064nm in three powers (35,40and 80 mW). The Nd:YAG laser is very common because of its features: simple construction, reliability and large variability. The characteristics of Nd:YAG laser are listed in Table (3.2).

Table (3.2) Characterization of Nd:YAG laser

Physical and Chemical Properties	
Chemical Formula	$Nd:Y_3A1_5O_{12}$
Melting Point	1970°C (2243K)
Density	4.56 g/cm^3
Refractive Index	1.82
Physical and Optical properties	
Lasing Wavelength	(532,1064) nm
Radiative Lifetime	550 ms
Divergence angle	0.625 mard
Linewidth	0.6 nm

3.3.1.2 The Detector

The detector was putting after the aperture to measure the output energy of laser in Z-Scan technique. This instrument is shown in figure (3.3), while the general specification of the detector are listed in Table (3.3).

Table (3.3)The general specification of the detector

Measuring range	40μW, 400μW,4mW, 40mW
Wavelength range	190 nm to 1100nm
Wavelength	633nm(He-Ne laser) reference wavelength convert by a table of spectral sensitivity characteristic(representing value)
Optical sensor	Si photodiode(Φ9mm)
Display	Numeric : 3999 full scale, Bargraph : 42 segment
Over display	The character 4 appears in the highest digit
Sampling rate	Approx. 2 times/sec. for numeral display, Approx. 20 times/sec. for bar graph.
Operating temperature / humidity	0°C ~ 40°C, 80%RH(Max) No condensation
Storage temperature / humidity	-10°C ~ 50°C, 80%RH(Max) No condensation
Environmental condition	Altitude 2000m or below, pollution degree II
Power consumption	Approx. 6mW
Safety standards	IEC61326-1
Battery	LR44 x 2
Size / Mass	Main body : H117 x W76 x D18mm/approx. 120g Sensor probe : H 84 x W16 x D10mm
Standard accessories included	Instruction manual

Figure (3.3) laser power meter (detector)

3.4 The Lithium Triborate crystal

Nonlinear single crystal LBO II is widely used as the third harmonics generators for Nd:YAG lasers 1064 nm. The LBO crystal was placed on a suitable holder in front of the Nd:YAG laser, and aligned with the same axis of the Nd:YAG laser rod using the He:Ne laser beam to provide more accurate output. Some features and physical properties of LBO crystal are listed in Table (3.4).

Table (3.4) Specification of LBO crystal

Physical Properties	
Productive company	Atom Optics Co., Ltd. (Chinese Academy of Sciences)
Chemical formula	LiB_3O_5
Transparency Range	$(0.16 – 2.6)$ µm
Size	$(5.95 \times 5.95 \times 5.95)$ mm^3
Optical symmetry	negative biaxial
Flatness & wavefrom	$< \lambda/8$ at 633nm

Features of LBO single crystal
Wide transparency region
Type I and type II non-critical phase-matching (NCPM) in a wide wavelength range
High damage threshold
Wide acceptance angle and small walk-off angle
High optical homogeneity ($\delta n = 10^{-6}$/cm)

3.5 Harmonics Generation Setup

Assuming a plane wave and non-depleting fundamental power, the Harmonics Generation output power was measured for different incident angles in the range from -30° to 30° increments of 5°step as shown in figures(3.4) and (3.5) respectively. The measurements of intensity based on one value of LBO crystal thickness 5.95mm. The incident angle of fundamental beam was changed by tilt the crystal forward to the left of the optical axis to make a positive angle, and backward to the right of the optical axis to make a negative angle. Bevel protractor was used to measure the incident angle as it is seen in Fig. (3.6) and the Fig. (3.7) explain the diagram of THG measurements.

Figure (3.4) The set-up of THG measurements at wavelength1064nm

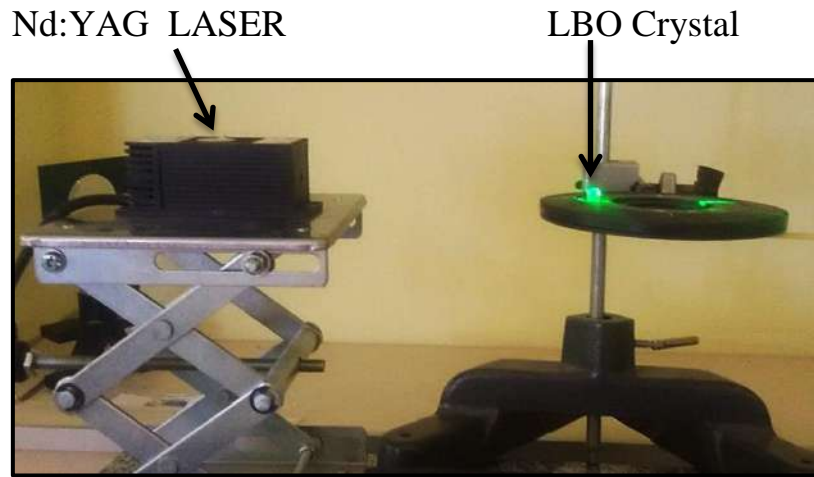Nd:YAG LASER   LBO Crystal

Figure (3.5) Generation of second harmonics from wavelength 1064 nm
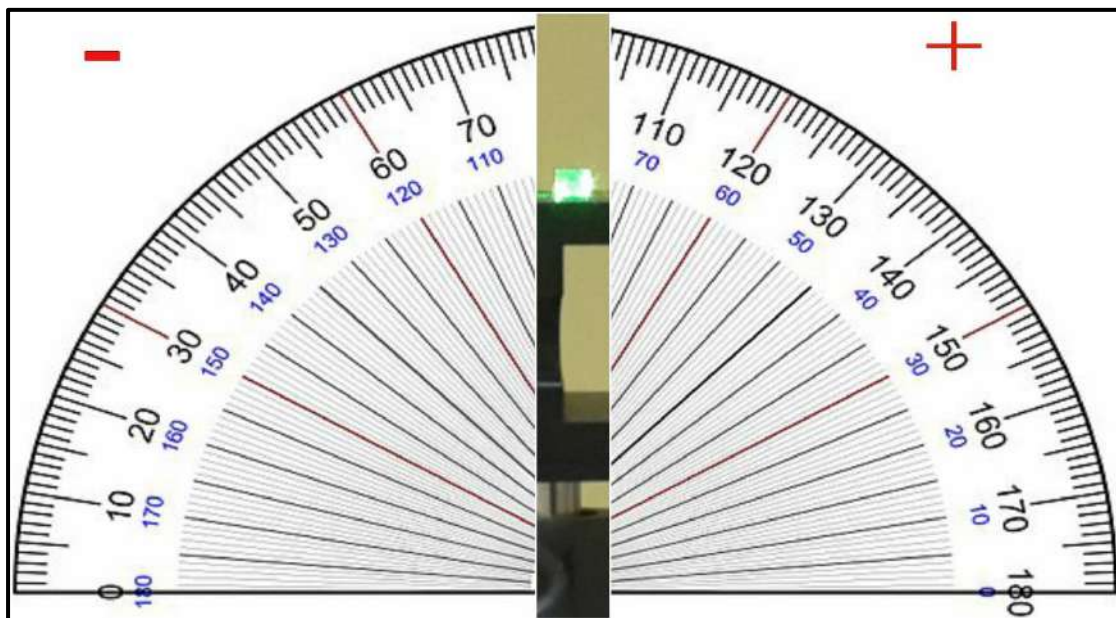Nd:YAG laser of input power 35mW

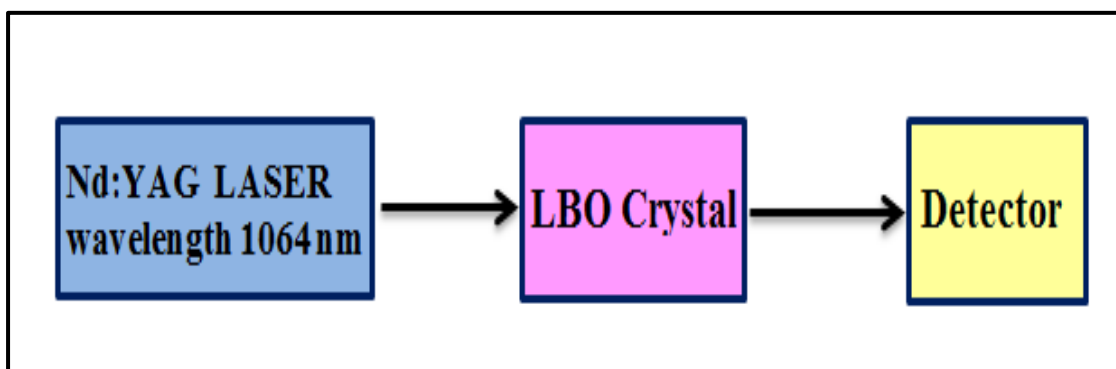Figure (3.6) 5.95mm crystal thickness tilts using bevel protractor.

Figure (3.7) Block-diagram of HG measurements.

CHAPTER FOUR

RESULTS

AND

DISCUSSION

4.1 Introduction

In this chapter, presented and discussed the experimental results for linear and nonlinear optical properties obtained of Lithium Triborate (LBO) single crystal. These results are included, absorption coefficient and refractive index in different wavelengths by means of Z-Scan technique. Z-Scan technique results are presented for two cases, closed and open aperture, and for each case, the wavelength used is 532 and 1064 nm, the results of the third harmonics generation intensity which are arranged by means of one and two steps are presented also .

4.2 Optical Properties for Lithium Triborate (LBO)

4.2.1 Linear optical properties experimentally

The linear optical properties for LBO crystal were studied, in two wavelengths 532 nm and 1064 nm respectively. This properties includes, transmittance, absorption coefficient, extinction coefficient, reflectance and refractive index which are explained in table (4.1).

Table (4.1)

Linear optical properties for lithium triborate (LBO) crystal

λ (nm)	t (cm)	T%	α_o (cm)$^{-1}$	$K \times 10^{-7}$	R	n
532	0.595	0.89	0.19585	8.29	0.05939	1.644456
1064	0.595	0.9	0.17707	15	0.05424	1.607223

4.2.1.1 Absorption Spectrum

The absorbance of LBO to incident radiation which was obtained directly from the spectrophotometer (UV-visible) at the wavelength range

from 190 to 1075 nm is recorded using Shimadzu (UV-1800) for constant thickness (5.95mm).The obtainable values of the absorbance were used in calculating and estimating other required parameters. It can be observed from Fig.(4.1) that the LBO crystal have a very high absorbance in the wavelengths 190, 215 and 225 nm, then the absorbance is rapidly decreased with increasing of the wavelength. On most of the diagrams you will come across, the absorbance ranges from 0 to 1. The absorbance of 0 at some wavelength means that no light of that particular wavelength has been absorbed. The intensities of the crystal and reference laser beam are both the same, so the ratio I_o/I is 1. Log_{10} of 1 is zero(Beer's law), while the absorbance of 1 happens when 90% of the light at that wavelength has been absorbed, which means that the intensity is 10% of what it would otherwise be. In that case, I_o/I is (100/I0=10) and log_{10} of 10 is 1.
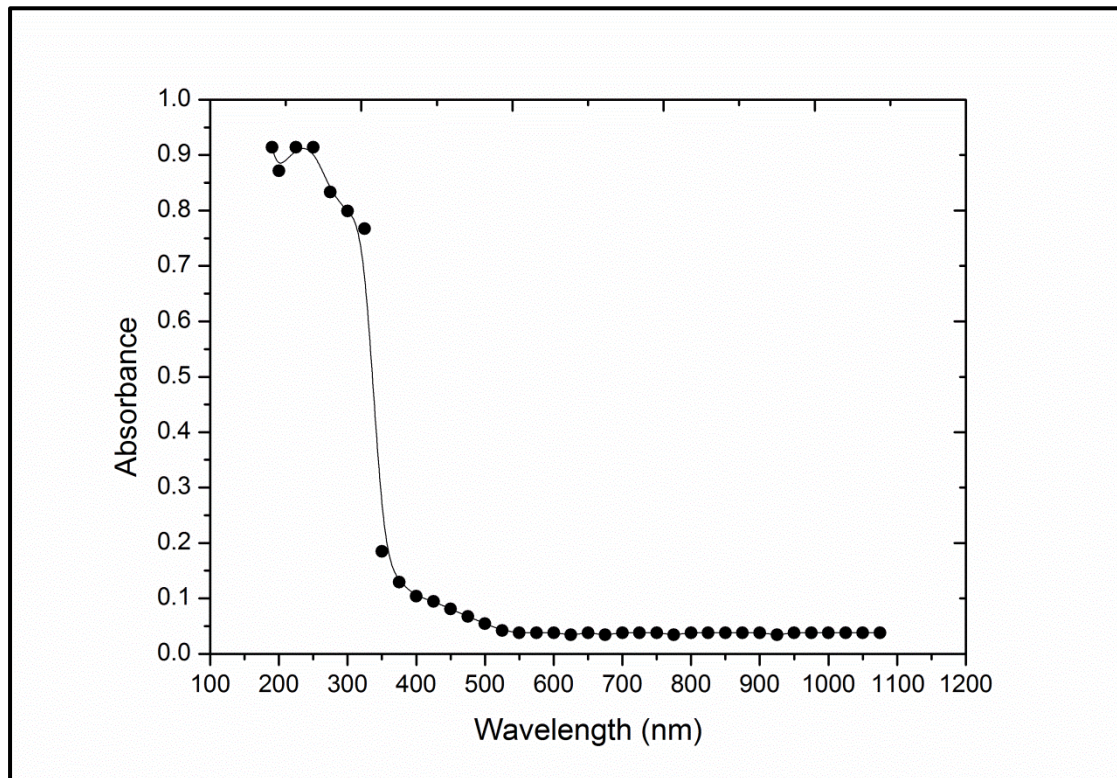

Figure (4.1) Absorbance against wavelength for LBO crystal

4.2.1.2 Linear Absorption coefficient (α_o)

The linear absorption coefficient (α_o) of a crystal is a property of the crystal which explained the amount of light absorbed. Thus, if a material shows a high absorption coefficient, it suggests that much laser light will be absorbed by this material which in turn, could make the material a potential absorber for Harmonics Generation. The linear absorption coefficient depends on the energy of the photon and the type of the electronic transitions that occur between energy bands, so according to this point the results will be approximate conceive of the structure of energy band. The linear absorption coefficient is determined from equation (2.6) for LBO crystal at wavelengths(532 and 1064) nm respectively. Fig.(4.2) shows a very high value of the absorption coefficient (3.53 – 0.13) cm $^{-1}$ and it is still increases as the photon energy increases. It can be observed from the figure that the maximum value of the absorption coefficient being 3.538cm^{-1} obtained at photon energy 4.96eV. Since LBO crystal described by high absorption coefficient (between 3.8eV to 6.5eV).
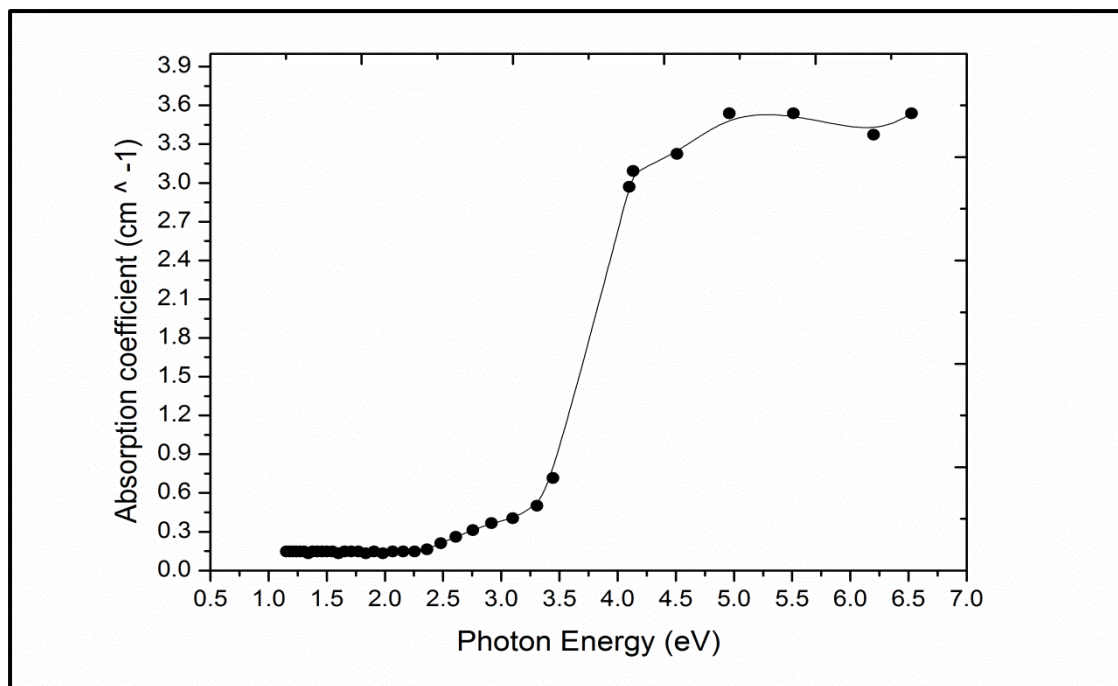

Figure (4.2)Absorption coefficient against photon energy.

4.2.1.3 Extinction Coefficient

First observation on the Fig. (4.3), this figure of the extinction coefficient is almost similar to the Fig. (4.2) of the absorption coefficient because of the first coefficient depend on the second one as in the equation (2.10), from this equation the extinction coefficient is determined. On the other hand, Fig. (4.3) reveals that the extinction coefficient of the LBO decreases gradually to the point where the photon energy is (2.75 eV) and thereafter increases steadily. However, The extinction coefficient for the crystal is seen to increase gradually as the photon energy increases, reaches a maximum and thereafter, decreases with photon energy. The maximum value of extinction coefficient (7.38×10^{-6}) obtained at photon energy of (4.13 eV).
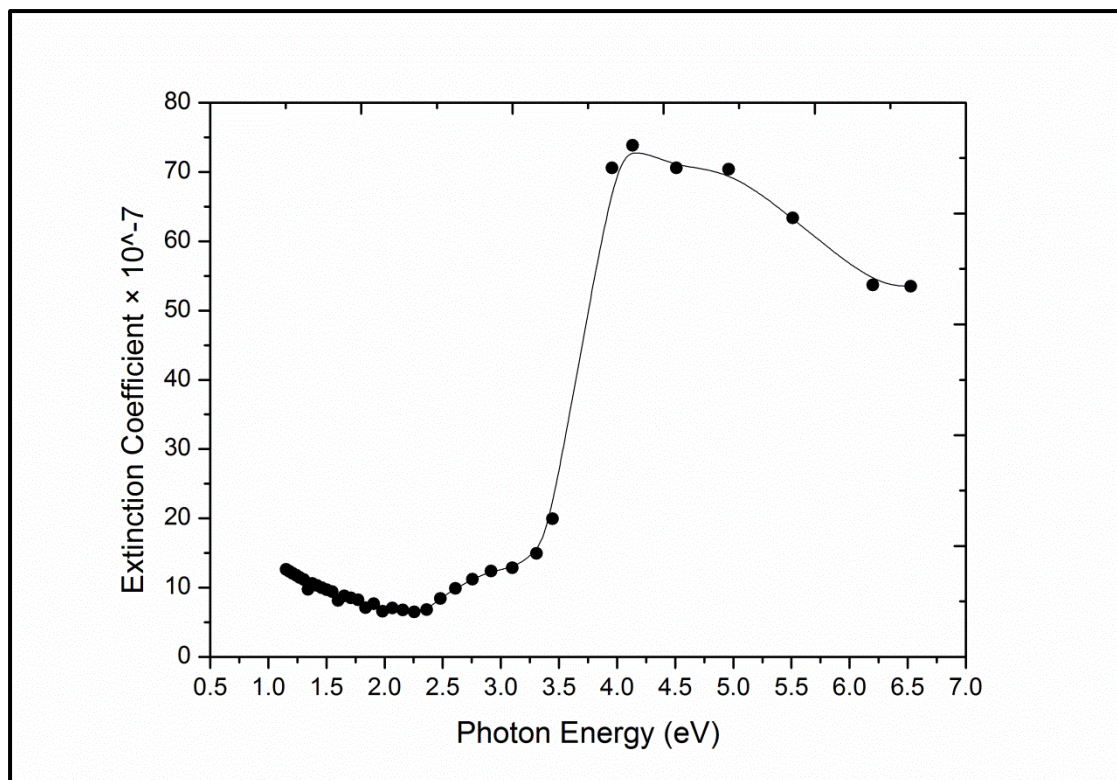
Figure (4.3)Extinction coefficient versus incident photon energy.

4.2.1.4 The Linear Refractive Index

Figure (4.4) explains how the refractive index of the crystal varies with the photon energy. The refractive index determined from equation (2.8). LBO was found to possess high refractive index (between 1.14 - 2.15). This also confirms LBO to be a good material for fabrication of optical waveguides.
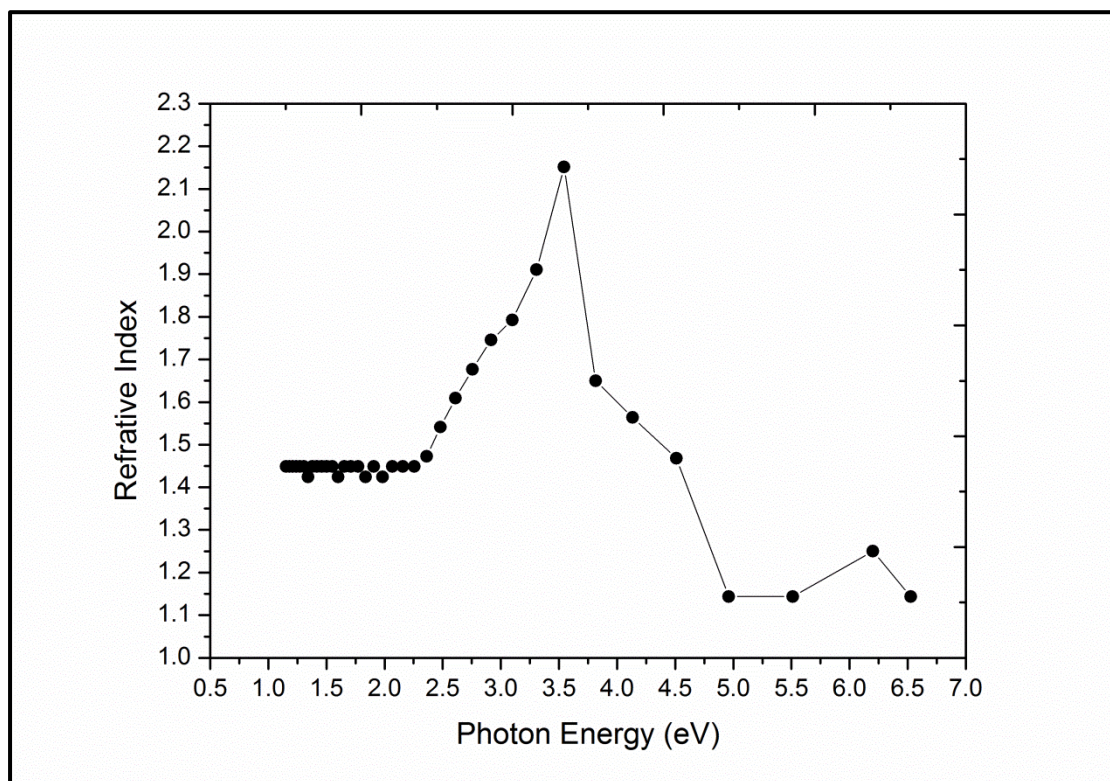
Figure(4.4) Refractive index versus wavelength of incident radiation.

4.2.1.5 The Reflectance

Figure(4.5) shows the gradually decrease of the reflectance curve of LBO crystal as photon energy increases. The maximum reflectance value was recorde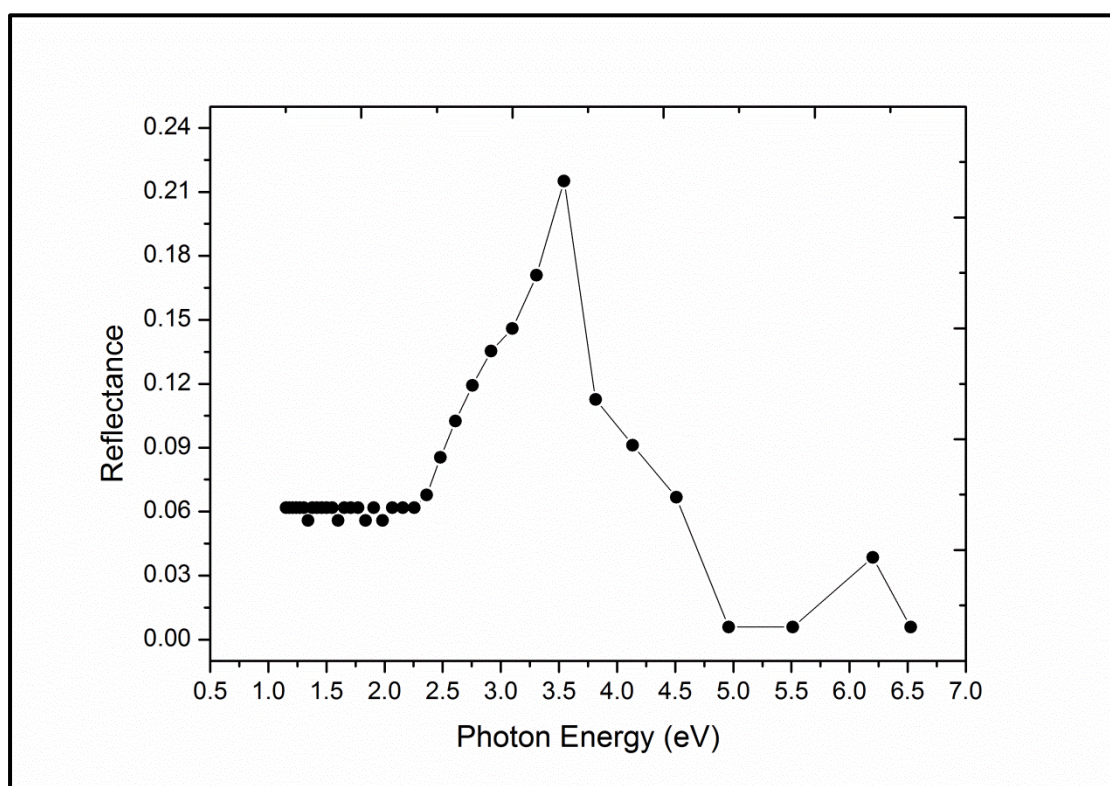d between (20% and 17%) in the photon energy range of (3.54-3.3)eV. This figure is almost similar to the figure (4.4) of the refractive index because of the first parameter depend on the second one as in the equation (2.8).


Figure(4.5) Reflectance spectra for LBO crystal

4.2.1.6 The Optical Conductivity

The optical conductivity spectrum of Lithium Triborate (LBO) crystal is as shown in Fig.(4.6). The value of this optical property is determined from equation (2.11), The figure was observed that the optical conductivity decreased in the high wavelength and increased in the low wavelength, this decrease is due to the low absorbance of the crystal .

The spectrum in Fig.(4.6) shows that the crystal was of high optical conductivity values which range from (1.17×10^8) to (1.08×10^8).
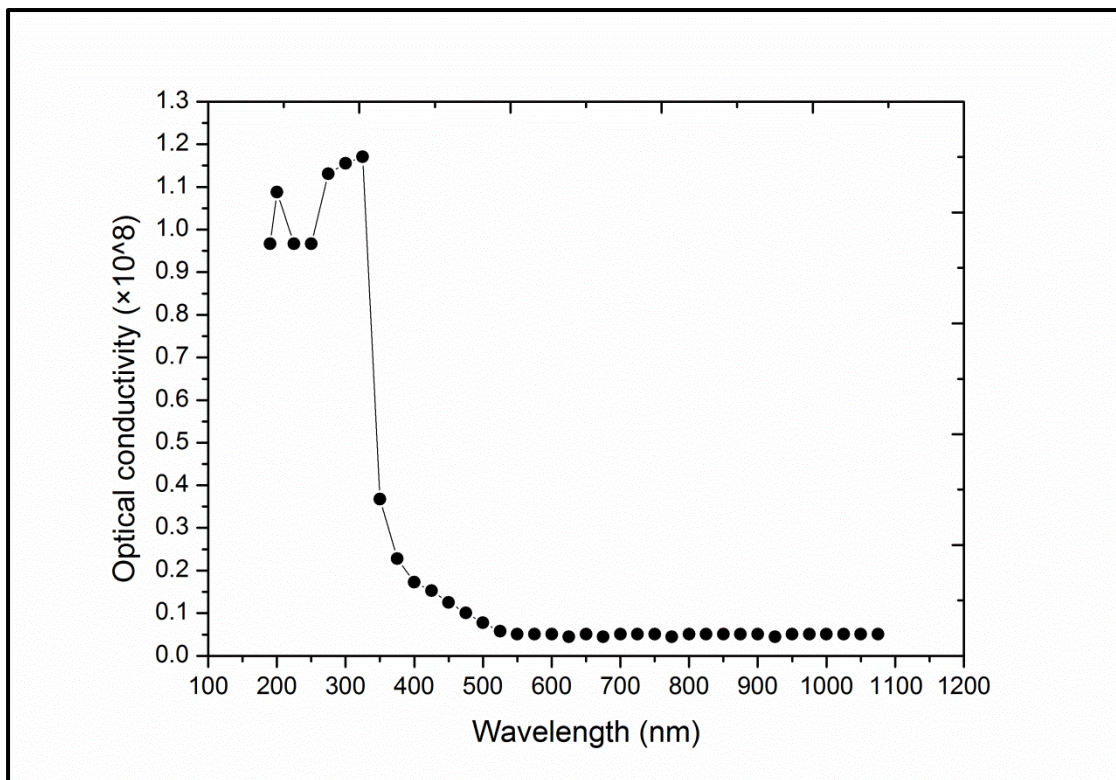
Figure(4.6) The optical conductivity versus the wavelength of incident radiation .

4.2.1.7 The Dielectric Constant(ε)

The real ε_1 and imaginary ε_2 part of the dielectric constant are determined from equations (2.13) and (2.14) respectively. These values depend on the wavelength were shown in Figures(4.7) and (4.8) respectively. The ε_1 values are higher than that of ε_2 values. It is seen that

the ε_1 and ε_2 values increase with increasing the wavelength and then decreasing with it.
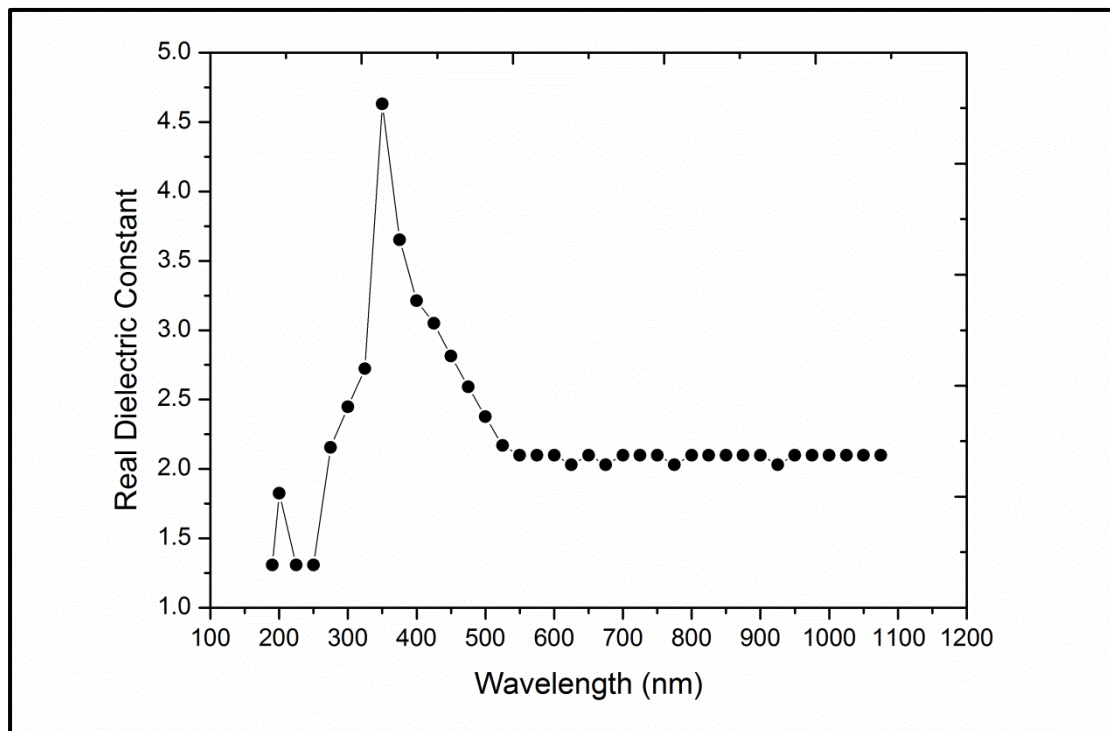

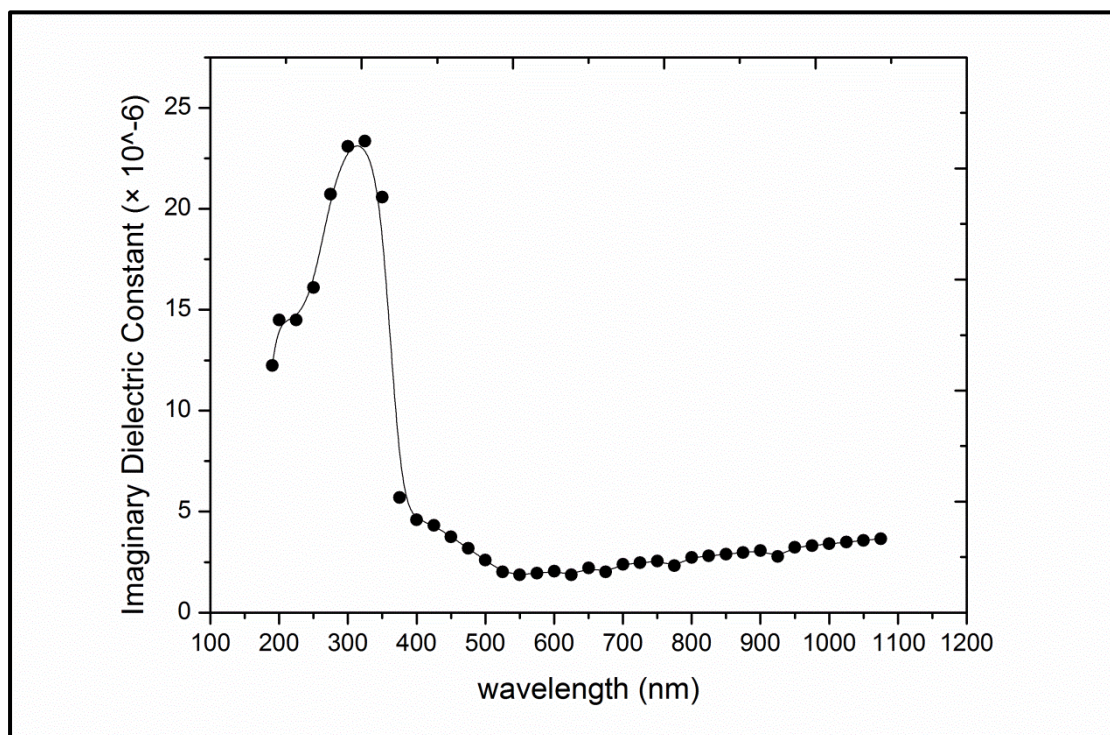Figure (4.7) Dependence of real dielectric constant on the wavelength.

Figure (4.8) Dependence of imaginary dielectric constant on the wavelength.

4.2.1.8 The Band Gap Energy

The band-gap energy, obtained when the absorption coefficient squared multiply by photon energy were plotted against the photon energy as shown in Fig.(4.9) below. The point of the linear part of the plot extrapolated to intercept the photon energy axis gives the value for the band gap energy. The value was found to be 2.125eV. The band gap arise from two causes, the linkage of the anionic groups in the LBO crystal and reduced conjugated bonding in the borate anionic groups. LBO crystal consists of $(B_3O_7)^{5-}$ anionic groups which are linked throughout the crystal and contain both trigonal and tetrahedral coordinated boron-oxygen bonding. These structural differences result in partially removes the conjugated bonds associated with trigonal coordinated boron-oxygen bonding in the anionic groups, thereby decreasing the band-gap energy.
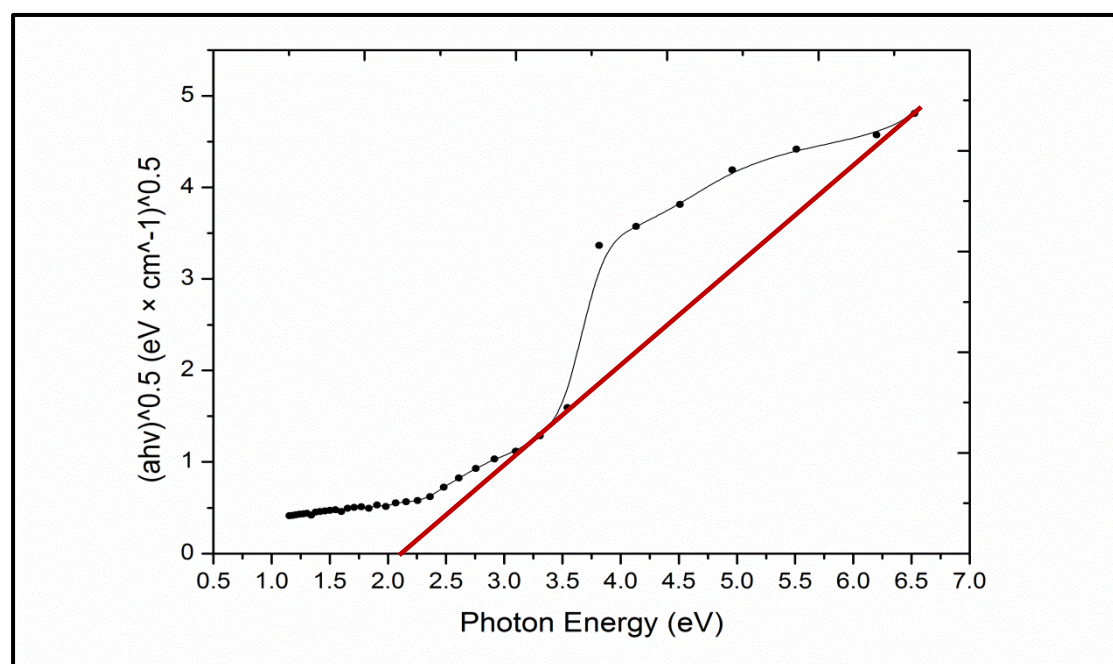
Figure(4.9) The variation of the $(\alpha h\nu)^{0.5}$ with the incident photon energy.

4.2.2 Linear Optical Properties Theoretically

In order to reproved our Lithium Triborate (LBO) model results for high good conditions as harmonics generation element , the dependence of the refractive index on the wavelength and the suitable range of angles incident for the reflectance in order to phase matching conditions obtain with high possibility .

The programming on the international data (Refractive index database) are applied as sketched in the Figures (4.10) and (4.11) respectively .
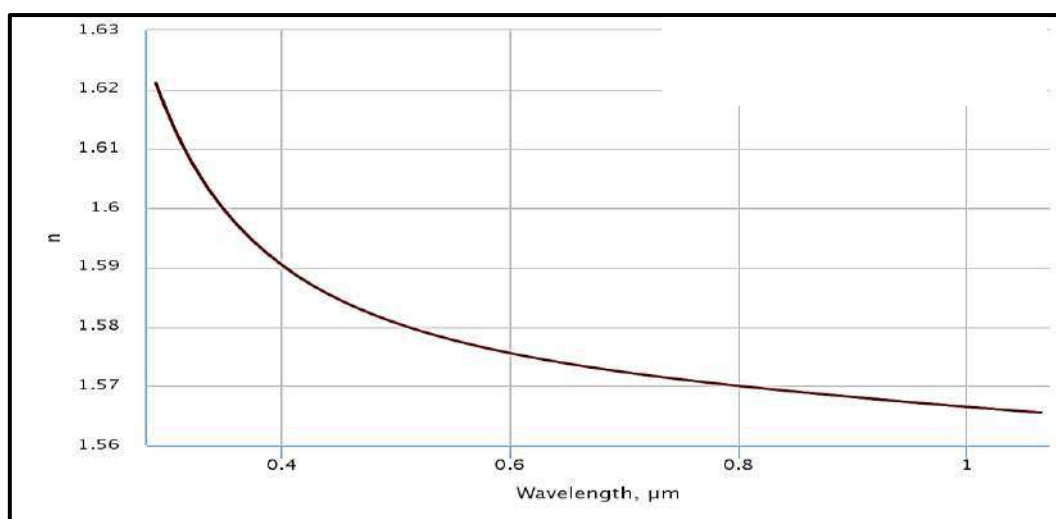

Figure (4.10) Dependence of refractive index on the wavelength

Figure (4.10) shows that refractive index of the LBO decreases gradually with the increased of the wavelength, at the 532 nm the refractive index was 1.5787 and 1.5655 at wavelength 1064 nm ,which is in agreement with our experimental results.
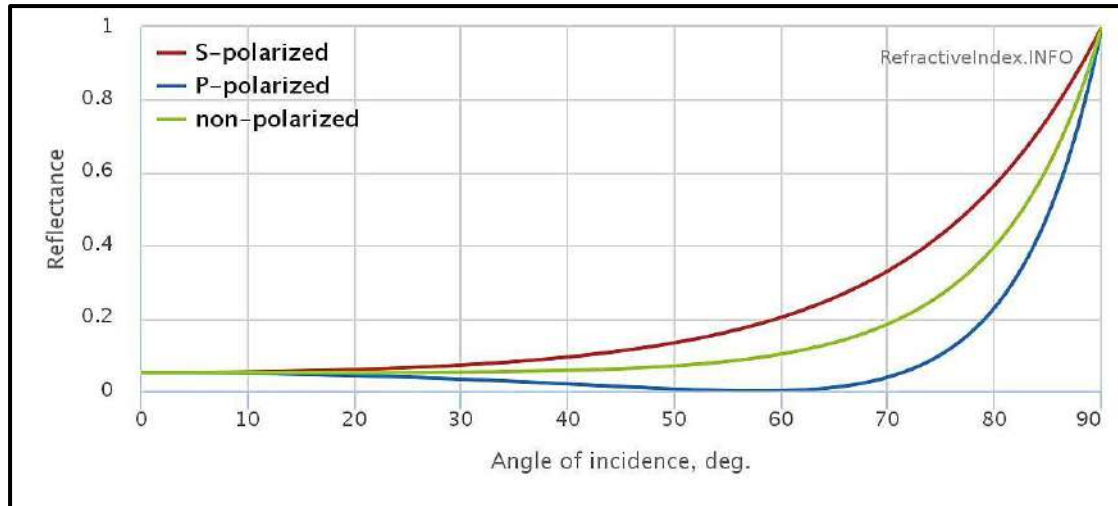
Figure (4.11) Dependence of reflectance on the angle of incident

Also can be observed from Fig. (4.11) that the reflectance from the incident face of LBO crystal are $(40)^o$ degree no more than 15% which is very satisfied for our goal.

4.2.3 Nonlinear optical properties

The nonlinear optical properties were investigated for model Lithium Triborate (LBO) crystal with thickness of (t=5.95mm) by mean of powers (P = 25 & 40 mW) at (532 and 1064 nm) of Nd-YAG laser. This properties includes nonlinear refractive index n_2 and nonlinear absorption coefficient β are listed in table (4.2).

Table (4.2)
The results of nonlinear optical properties for lithium triborate (LBO) crystal by the Z-Scan at different laser powerful(25mW and 40mW) .

λ $\times 10^{-7}$ (cm)	ΔT_{p-v}	Power of laser (mW)	I_o (mW/cm^2)	$\Delta\emptyset_o$ (Rad)	$n_2(\dfrac{cm^2}{mW})$ $\times 10^{-9}$	T_{max}	$\beta\,(\dfrac{cm}{mW})$ $\times 10^{-3}$
532	4.02	25	49100	9.9	3.04168	30.85	3.727
	3.92	40	78600	9.65	1.85281	36.34	2.328
1064	0.66	40	78600	1.62	0.62049	36.5	2.326

4.2.3.1 Nonlinear Refractive index measurements

The nonlinear refractive index (n_2) of Lithium Triborate (LBO) crystal was measured experimentally by the results of the closed aperture Z-Scan technique. The nonlinear refractive index can be determined from the curve of the normalize transmission figures (4.12,4.13 and 4.14) respectively by using equation (2.2). This figures shows the relation between the normalize transmission T(z) and the position (Z) of the LBO crystal by a closed aperture Z-Scan technique at two different laser wavelengths (532nm and 1064 nm)with different laser powerful (25mW ,40mW) respectively.

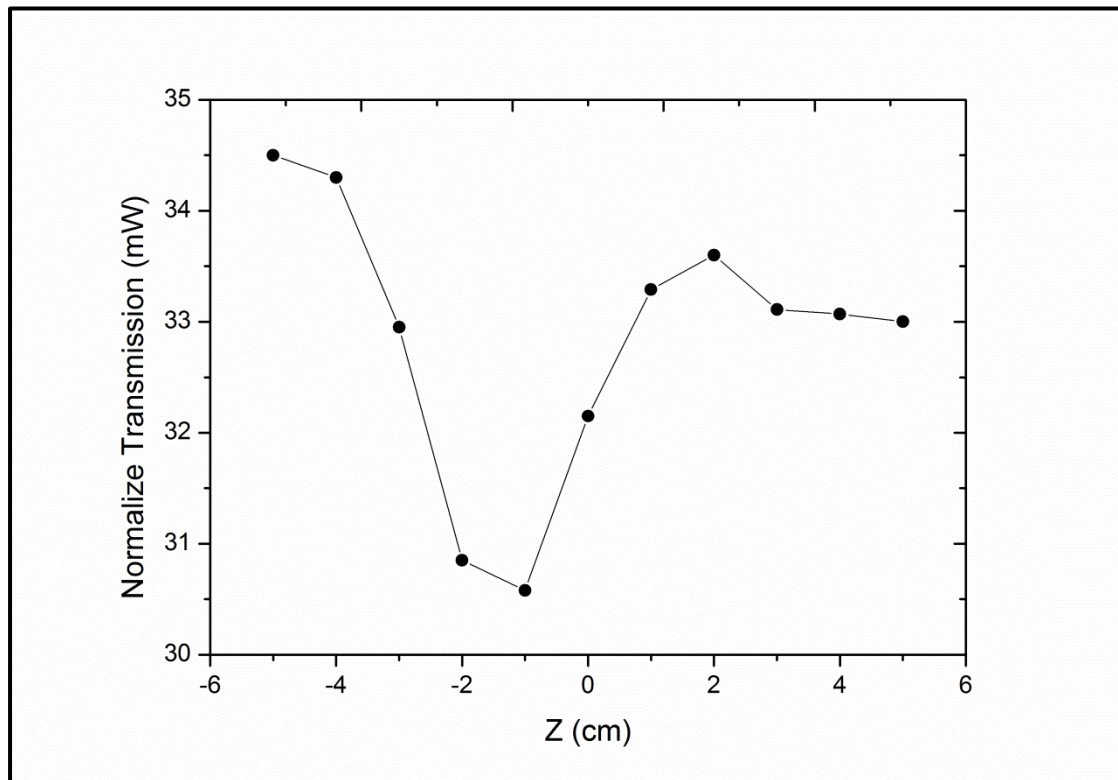Figure (4.12) Closed aperture Z-Scan for LBO in wavelength 532 nm at 40 mW

In figure (4.12), the nonlinear effect region is extended from (-5)to (5)cm, the valley-peak configuration indicates the positive sign of refractive index nonlinearity $(+n_2)$ self-focusing.
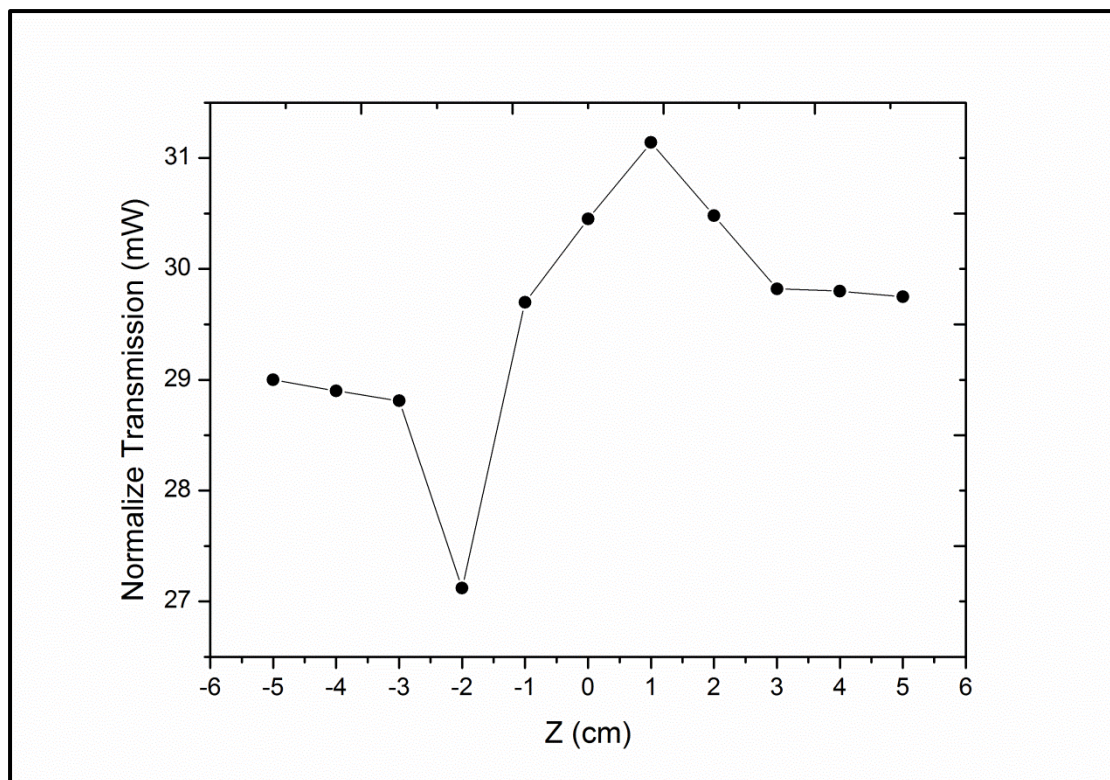
Figure (4.13)Closed Aperture Z-Scan for LBO in wavelength 532 nm at 25 mW
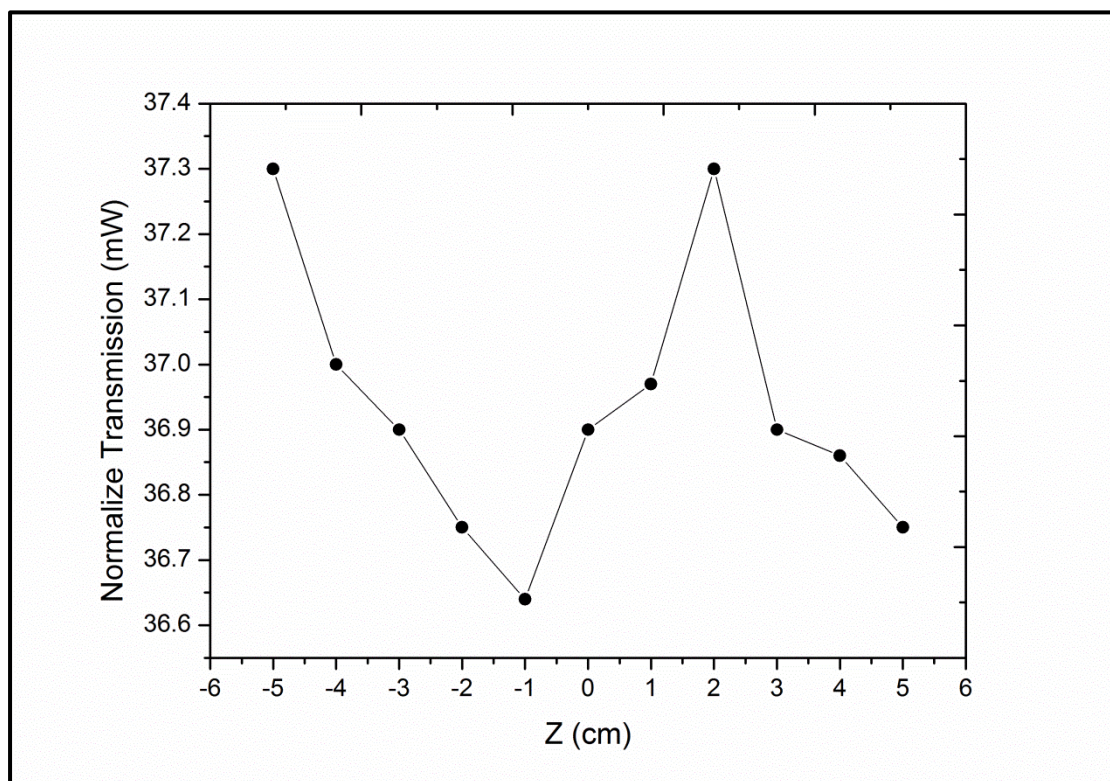
Figure (4.14) Closed aperture Z-Scan for LBO in wavelength 1064 nm at 40 mW

Figures (4.13 and 4.14) shows the normalized transmittance for the closed aperture (CA) curve of LBO. The valley to peak configuration of the curves indicates that the sign of the nonlinear refractive index is positive ($n_2 > 0$), exhibiting a self-focusing effect. This may be an advantage for the application in protection of optical sensors. As seen from the closed aperture Z-scan curve, the prefocal transmittance valley is followed by the post focal peak which is the signature of positive nonlinearity.

4.2.3.2 Nonlinear Absorption coefficient

The nonlinear Absorption coefficient (β) of LBO was measured experimentally by the results of the open aperture Z-Scan technique. The nonlinear Absorption coefficient can be determined from the curve of the normalize transmission figures (4.15, 4.16 and 4.17) respectively by using equation (2.7). This figures shows the relation between the normalize transmission T(z) and the position (Z) of the LBO crystal by open-aperture Z-Scan technique for LBO crystal at different laser wavelengths (532nm and 1064nm) with different laser powerful(25mW, 40mW) respectively.

As it is seen in Figures (4.15) and (4.16) the peak of the normalize transmission curve indicates that the LBO crystal exhibited saturation absorption.
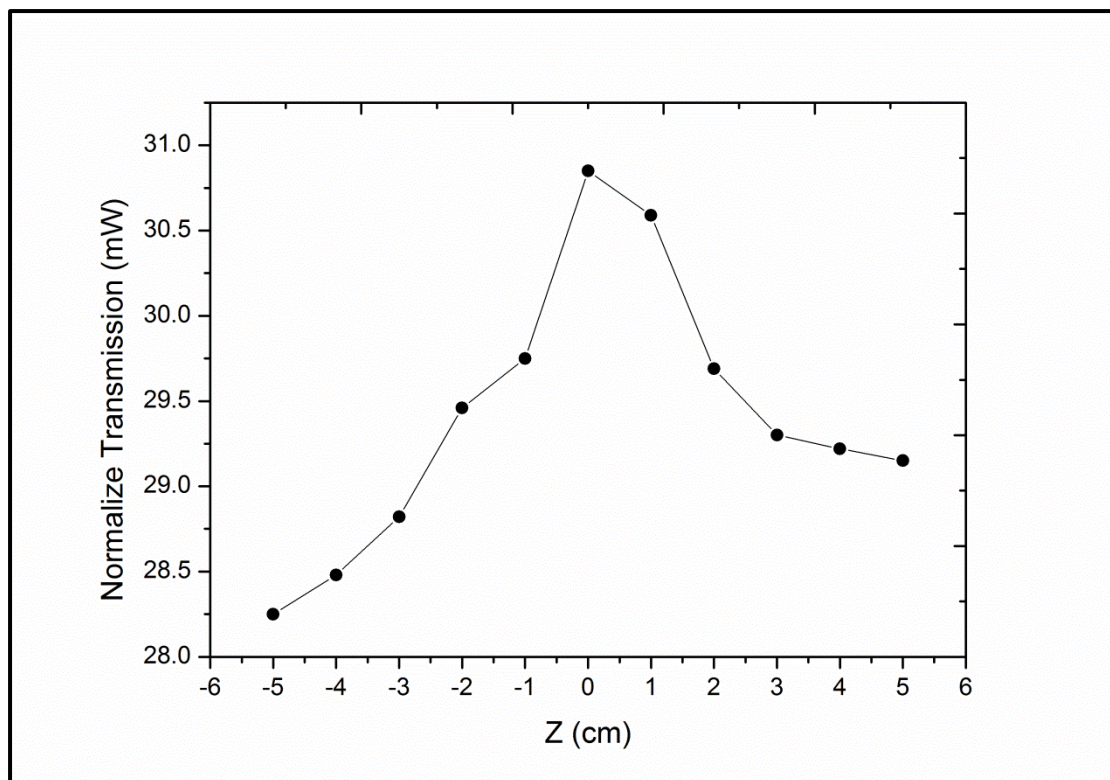
Figure (4.15) Open aperture Z-Scan for LBO in wavelength 532 nm at 25 mW
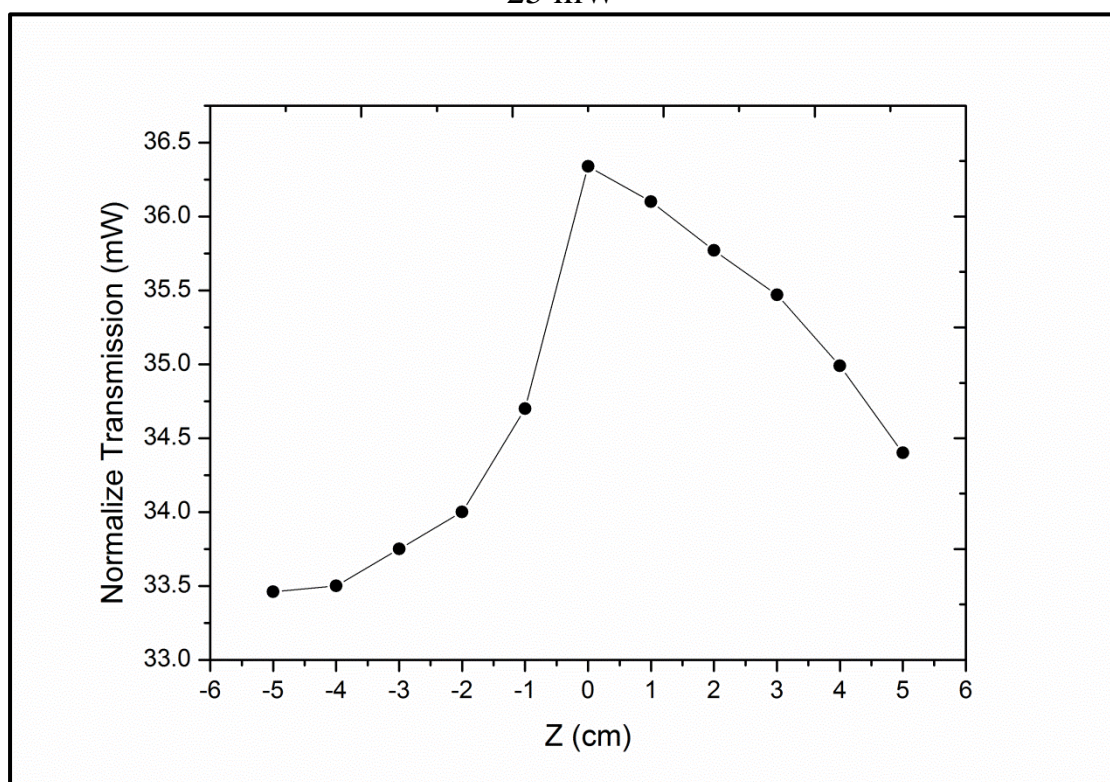
Figure (4.16) Open aperture Z-Scan for LBO in wavelength 532 nm at 40 mW

Figure (4.17) showed that the valley of the normalize transmission curve indicates that the LBO crystal exhibited two photon absorption.
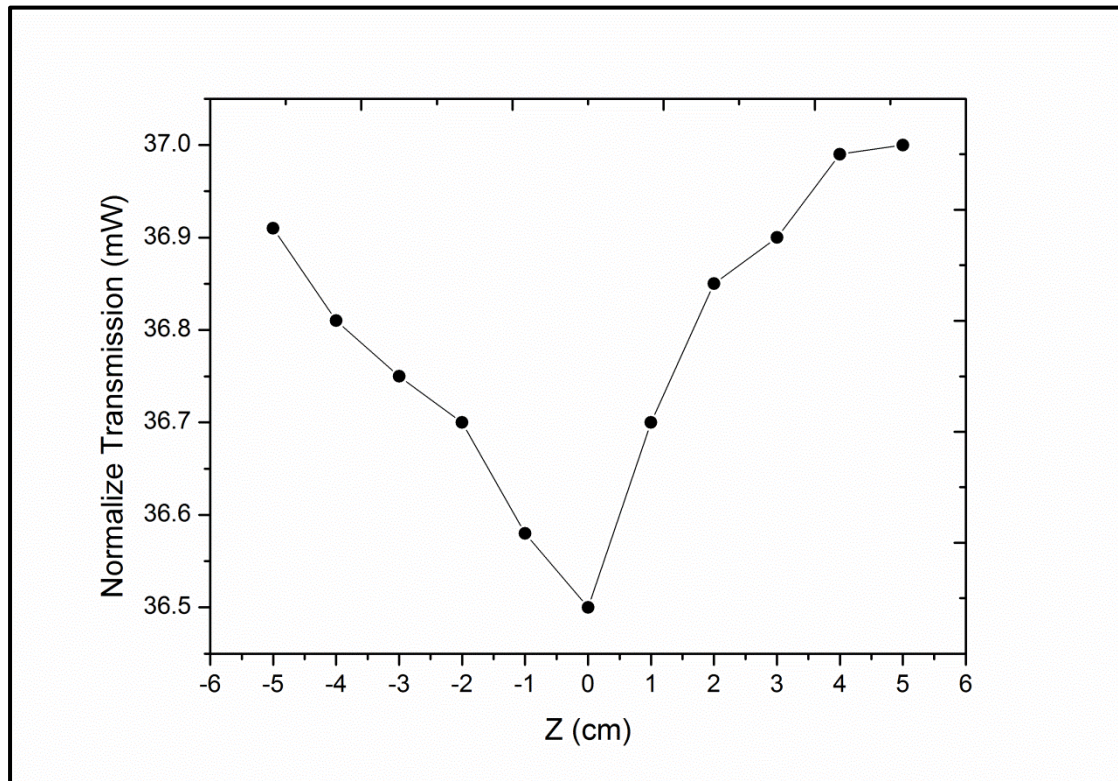
Figure (4.17) open aperture Z-Scan for LBO in wavelength 1064 nm at 40 mW

4.3 The Intensity of Harmonics Generation (SHG & THG):

From experimentally results the figure (4.18), shows low Harmonics Generation intensity obtained at the angles -20° and 25°. The reason of this effect is the high re-absorption of Harmonics generation beams in the LBO crystal at these angles. Furthermore, the path length inside the crystal was decreased when increasing the incident angle. Harmonics generation intensity was vanished at the critical incident angles, which was obtained at -30° and 30° because no signal will be detected at the critical angles.
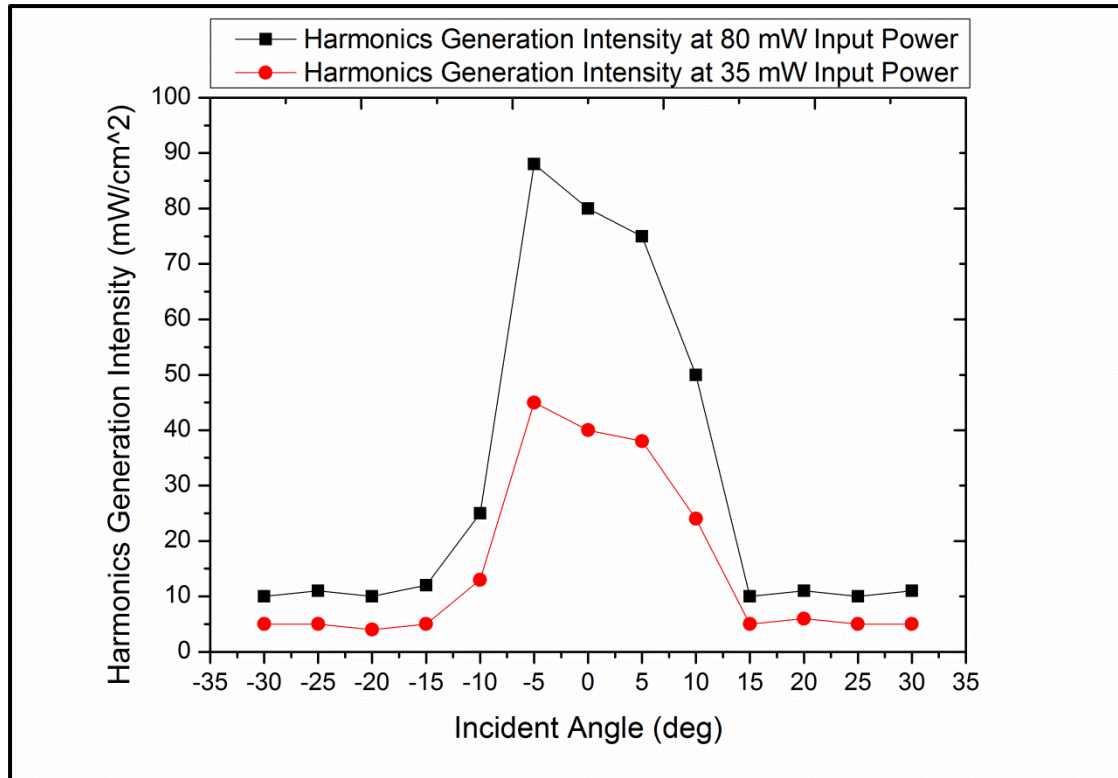
Figure (4.18) Harmonics generation output intensity excited at
(80 and 35) mW input power for 1064 nm versus incident angle

The results showed different values of Harmonics generation intensity at each input power due to the change in the incident angle of fundamental beam. The reason of the change in the incident angle of the fundamental beam is to obtained the efficient Harmonics Generation intensity. The change in the incident angle of fundamental beam was induced a change in refractive index which is well agreement with our theoretical results shown in Fig.(4.10).When the input power of 1064 nm Nd-Yag laser was 80mW the generated of the Third Harmonics by using LBO crystal was obtained at incident angle 18 ^{o} with 32 mW powerful, While the Second Harmonics Generation was obtained at incident angle 18° with 12 mW when the power of Nd: YAG laser 1064 nm was 35 mW.

The efficiency of harmonics generation can be calculated from Eq. (2.15) and (2.18) , It can be observed from the results in table (4.3),

that the efficiency of the LBO crystal to generated third harmonics by two step technique is greater than the efficiency that generated the second harmonics.

Table (4.3): The efficiency of high harmonics generation

Laser type	Input Power	Harmonics Generation	The efficiency%
Nd:YAG 1064 nm	35	SHG	30
Nd:YAG 1064 nm	80	THG	70

The optimum value of THG intensity was found by using Eq. (2.17) for each input power as listed in table 4.4:
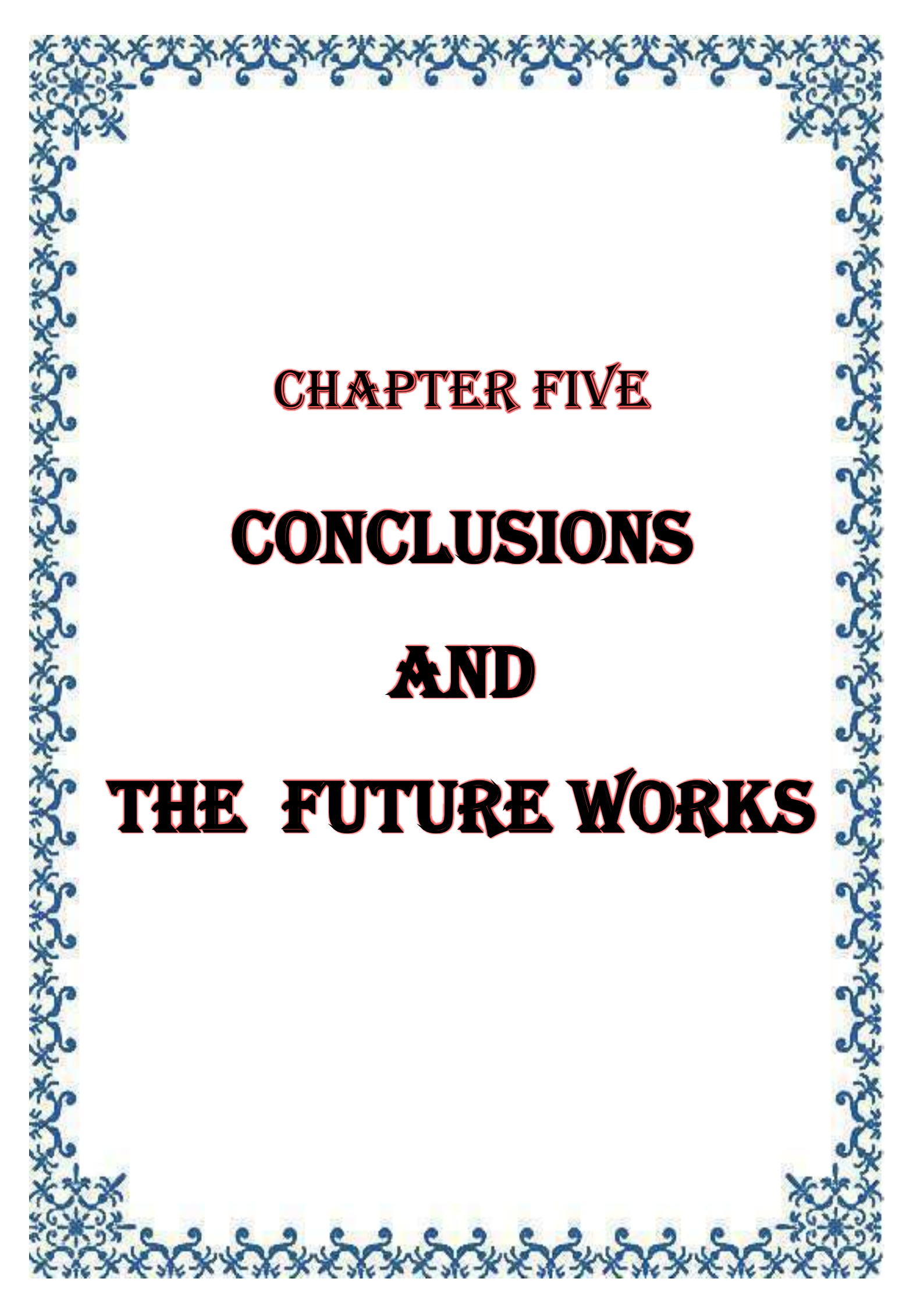
Table (4.4): THG intensity excited at (80 and 35)mW input power

Input Power (mW)	$I_\omega \times 10^3$ (mW/cm^2)	Optimum value of $I_{3\omega} \times 10^{11}$ (mW/cm^2)
35	68.8	1.04
80	157.2	7.33

Table (4.5) explain the results of the nonlinear optical susceptibility from its real and imaginary part, for two input power (25 and 35) mW are calculated by using equations (1.7), (1.8) and (1.9).

Table (4.5): The results of the third order nonlinear optical susceptibility

Power (mW)	Incident Intensity (mW/cm^2)	Re. χ^3 (cm^2/W)	Im. χ^3 (cm^2/W)	χ^3
25	49100	6.95×10^{-7}	3.06×10^{-13}	6.95×10^{-7}
37	72737	6.64×10^{-7}	4.65×10^{-13}	6.64×10^{-7}

CHAPTER FIVE

CONCLUSIONS

AND

THE FUTURE WORKS

5.1 Conclusions

After obtaining practical results that determine the optical properties and the harmonics intensity of the LBO crystal, The concluded of the results are described below:

5.1.1 The results show that the absorption spectra of lithium triborate to incident radiation is suitable to apply for difference nonlinear optics phenomena.

5.1.2 The observation for the results between the transmission and the distance (Z), can be used to determine the type of the crystal to be convex or concave.

5.1.3 The results show that the transmission is directly proportional with the wavelength, therefor, this material is excellent for the second and higher harmonics generation to convert the Ultraviolet frequencies to the visible and Infrared ranges respectively.

5.1.4 The most effective parameters that influence on the efficiency of the LBO crystal, as element for production harmonics generation, are the phase – matching condition and the temperature variations.

5.1.5 The results obtained for harmonic energies and the conversion efficiencies indicated the LBO type II crystal is satisfy to production third harmonics generation in the range of Ultraviolet range with two steps without need an extreme intensive lasers.

5.2 Future works

5.2.1 Experimental study on optimum efficiency of LBO crystal for higher harmonics generation (HHG) with other intensive Lasers.

5.2.2 Investigate to optimize the performance of this proposal crystals sample as the element for Q-switching solid-state laser with high power pulsing.

5.2.3 Study on optimization methods to compensate the effect of the ray-walk off and temperatures fluctuations by suitable incident rays and thermal tuning investigations.

5.2.4 Simulation study on the nonlinear optical properties of LBO crystal to prepare the three – wave mixing .

5.2.5 Using Y-Scan technique to find the optimum phase – matching conditions for some nonlinear effect.

5.2.6 Study on using LBO crystal to combination the optical parametric oscillator of both type I and type II phase-matching, with the second harmonics generation.

5.2.7 Study on the performance of LBO crystal as optical limiter with different laser wavelengths and optical input powers respectively.

REFERENCES

References

[1] Robert W. Body, "Nonlinear Optics", Third Edition , Rochester, New York, (2007).

[2] S.R. Marder et al., "Materials for Nonlinear Optics, Chemical Perspectives, ACS Symposium Series 455",American Chemical Society, Washington DC, (1991).

[3] P.A. Franken A. E. Hill, C.W. Peters, and G. Weinreich , "Generation Of Optical Harmonics, Physical Review. Letters", 1961, 7(4), PP 118.

[4] T.H. Maiman, "Stimulated Optical Radiation in Ruby", Nature, 1960, Vol.187, No. 4736, PP 493-494.

[5] Frank Träger , "Handbook of Lasers and Optics", second edition, Germany, (2012).

[6] Richard L. Sutherland, "Hand Book of Nonlinear Optics" , second edition , Dayton, Ohio , U.S.A., 2003 , p1.

[7] Ronald W. Waynant , Marwood N. Ediger ,"Electro-Optics Handbook", second edition, Rockville, Maryland, P 478, (2000).

[8]Amnon Yariv, Pochi Yeh , "Optical waves in crystals propagation and control of Laser radiation", California,(1983).

[9] Henrik Enqvist , 2004, "A setup for efficient frequency tripling of high-power femtosecond laser pulses", Thesis , Lund Reports on Atomic Physics, LRAP-330, Lund, PP4,26.

[10] Bearbeitet von, Chuangtian Chen, Takatamo Sasaki, Rukang Li, Yincheng Wu, Zheshuai Lin, Yusuke Mori, Zhangui Hu, Jiyang Wang, Masashi Yoshimura, Yushi Kaneda, "Nonlinear Optical Borate Crystals Principles and Applications", First Edition, (2012).

[11] Mihaela Balu, 2006, "Experimental Techniques For Nonlinear Material Characterization: A Nonlinear Spectrometer Using A White-Light Continuum Z-Scan", Thesis, University Of Central Florida, PP. 6.

References

[12] Nicolaas Bloembergen , "Nonlinear Optics , Nonlinear Optical Media" ,Chapter 8 .21.1.N.P 875, New York , (1965).

[13] Luca Rigamonti, Schiff Base, "Metal Complexes For Second Order Nonlinear Optics", Università Di Milano, (2010).

[14] Harry J. R. Dutton, "Understanding Optical Communications, International Technical Support Organization", First Edition,1998.

[15] Sergey A. Ponomarenko, "Fundamentals of Nonlinear Optics", Dalhousie university ,PP 77, (2015).

[16] Mark D. Peterson, Patrick L. Hayes, Imee Su Martinez, Laura C. Cass, Jennifer L. Achtyl, Emily A. Weiss, and Franz M. Geiger, "Second harmonic generation imaging with a kHz amplifier [Invited]", Optical Society of America, (2011).

[17] Marco Pizzocaro, Davide Calonico, Pablo Cancio Pastor Jacopo Catani, Giovanni A. Costanzo, Filippo Levi and Luca Lorini, "Efficient Frequency Doubling at 399nm", physics optics , arXiv:1401.1623v3 , (2014).

[18] G. Omar Clay, Andrew C. Millard, Chris B. Schaffer , Juerg Aus-der-Au , Philbert S. Tsai, Jeffrey A. Squier ,David Kleinfeld, "Spectroscopy of third-harmonic generation: evidence for resonances in model compounds and ligated hemoglobin", J. Opt. Soc. Am. B, Vol. 23, No. 5, (2006).

[19] Arne Potreck, 2014, "Nonlinear Optical Frequency Conversion for Lasers in Space", thesis, Eberhard-Karls Universität Tübingen, PP 43.

[20] J. M. Schins, T. Schrama, J. Squier, G. Brakenhoff, and M. Muller, "Determination of material properties by use of third-harmonic generation microscopy ", J. Opt. Soc. Am. B,Vol.19,No.7, PP 1627-1634 (2002).

References

[21] G. Peramaiyan , P. Pandi , V. Jayaramakrishnan , Subhasis Das , R. Mohan Kumar, "Investigation on second and third order nonlinear optical, phase matching and birefringence properties of g -glycine single crystals", Optical Materials, PP307-309 ,(2012) .

[22] D. von der Linde, K. Rzàzewski, "High-order optical harmonic generation from solid surfaces", Journal of Applied Physics B : lasers and optics, 63, PP 499-506, (1996).

[23] M. C. Kohler, T. Pfeifer, K. Z. Hatsagortsyan, and C. H. Keit,2012, "Frontiers of atomic high-harmonic generation", Germany.

[24] Kenichi L. Ishikawa, "High-Harmonic Generation", Photon Science Center, University of Tokyo.

[25]Amy Louise Lytle, 2008, "Phase Matching and Coherence of High-Order Harmonic Generation in Hollow Waveguides", thesis, University of Colorado, PP 2.

[26] Ba Khuong Dinh, 2012, "Phase-Matched High Order Harmonic Generation and Applications", thesis, Swinburne University of Technology, PP 10.

[27] Mar´ıa Moreno de Castro, 2009, "Control of light emission in Parametric Oscillators with Photonic Crystals", thesis, Universitat De Les ILLES Balears ,PP 4-5.

[28] M. S. Dresselhaus,2001, "Solid State Physics Part II Optical Properties Of Solids", PP135.

[29] Jonas Hellström, 2001, "Nanosecond optical parametric oscillators and amplifiers based on periodically poled KTiOPO$_4$", thesis, The Royal Institute of Technology, PP 6.

[30] Matthew Donald Seaberg,2014 , "Nanoscale EUV Microscopy on a Tabletop: A General Transmission and Reection Mode Microscope Based

References

on Coherent Di_ractive Imaging with High Harmonic Illumination", University of Colorado, PP 35.

[31] Michiel .J.A. de Dood, "Second-harmonic generation (how to get from a wavelength of 980 to 490 nm)", Huygens Laboratorium 909a,2006.

[32] Chuangtian Chen, Yicheng Wu, "New nonlinear-optical crystal: LiB_3O_5", J. Opt. Soc. Am. B,Vol. 6, No. 4, PP 616, (1989,).

[33] A. Borsutzky, R. Brünger , Ch. Huang , R. Wallenstein, "Harmonic and sum-frequency generation of pulsed laser radiation in BBO, LBO, and KD*P", Applied Physics B , Volume 52, PP 55-62, (1991).

[34] R. H. French, J. W. Ling, F. S. Ohuchi, C. T. Chen, "Electronic structure of β-BaB204 and LiB_3O_5 nonlinear optical crystals", PHYSICAL REVIEW B, VOLUME 44, NUMBER 16, (1991).

[35] XIE Fali, WU Baichang, MAO Hongwei, CHEN Chuangtian, "Efficient Generation of Deep Ultraviolet Radiation Using LiB_3O_5 Crystal", CHINESE PHYS. Lett. , Vol.9, No.5, (1991).

[36] G. C. Bhar, , P. K. Datta, , A. M. Rudra, "Non-collinear ultraviolet generation in a Lithium Borate crystal", Applied Physics B, Volume 57, pp 431-434, (1993).

[37] D. N. Nikogosyan," Lithium triborate (LBO)", Applied Physics A, Volume 58, PP 181-190, (2004).

[38] I. N. Ogorodnikov ,A. V. Kruzhalov and L. I. Isaenko, "Luminescent properties of crystalline lithium triborate LiB_3O_5", PHYSICS OF THE SOLID STATE, VOLUME 41, NUMBER 2 ,(1999).

[39] p.l. ramazza, s. ducci, a. zavatta, m. bellini1, f.t. arecchi1, "Second-Harmonic Generation from a picosecond Ti:Sa laser in LBO: conversion efficiency and spatial properties", Applied Physics B: LASERS and Optics , Vol. 75,pp 53–58 (2002).

References

[40] H.Q. Li, H.B. Zhang, Z. Bao, J. Zhang, Z.P. Sun, Y.P. Kong, Y. Bi, X.C. Lin, A.Y. Yao, G.L. Wang, W. Hou, R.N. Li, D.F. Cui, Z.Y. Xu, "High-power nanosecond optical parametric oscillator based on a long LiB3O5 crystal", Optics Communications 232, PP 411–415, (2004).

[41] Burcu Ardic¸og˘lu, Gu¨lhan Özbayog˘lu , Zeynep Özdemir, Ays¸en Yilmaz , Production and identification of rare-earth doped lithium triborate, Journal of Alloys and Compounds, 418, PP 77–79, (2006).

[42] Abdulnabi Hassan Mohsin, "Design and construction of a passively Q-switched Nd-YAG pumped UV laser and study its non-linear parameters", Thesis, University of Baghdad,2013.

[43] Burcu Ardiçoglu, 2005, "Synthesis of Rare-Earth Doped Lithium Triborate", Msc. Thesis, Middle East Technical University,p11.

[44]Arne Potreck, "Nonlinear Optical Frequency Conversion for Lasers in Space", Thesis, Eberhard-Karls Universität Tübingen, PP43,(2014).

[45]Nonlinear crystal Lithium Triborate, Eksma optics,
http://eksmaoptics.com/out/media/LBO_Crystals_Brochure.pdf

[46] Ae Ran Lim, Ji Won Kim and Choon Sup Yoon , "Local structure of LiB_3O_5 single crystal from 7Li nuclear magnetic resonance, Journal Of Applied Physics", Volume 94, Number 8,P1, (2003).

[47] Kostyantyn Sukhoy, 2011,"Generation of green second harmonic radiation in LBO, BBO, KTP, and PPLN crystals using passively Q-switched sub-nanosecond microchip laser", Thesis, University of Manitoba.

[48] Senthilkumar M, 2010, "Crystal Growth and Characterization of $La_2CaB_{10}O_{19}$, $Nd_xLa_{2-X}CaB_{10}O_{19}$and $K_2B_4O_{11}H_8$ for NLO and Laser applications and Theoretical Analysis of Nonlinear Optical Property of $La_2CaB_{10}O_{19}$ Crystal", Thesis, Anna University.

References

[49]   Tolga Depci, 2009, "Synthesis and Characterization of Lithium Triborate by Different Synthesis Methods and Their Thermoluminescent Properties", Thesis, Middle East Technical University .

[50] In Gyoo Kim and Sung Ho Choh, Jung Nam Kim, "NMR Study of ^{7}Li and $^{1}_{1}$B Nuclei in Nonlinear Optical LiB$_3$O$_5$ Single Crystal", Journal of the Korean Physical Society, Vol. 32, pp. S669_S671, (1998).

[51] I.N.Ogorodnikov, A.V.Kruzhalov, A.V. Porotnikov, Radiation resistance of nonlinear LiB3O5 crystals: optical properties" , PROC SPIE. V.2967, February 1997, Pages 120–125.

[52]Shen.Y.R ,"The principles of nonlinear optics", A Wiley-Interscience Publication John Wiley & Sons, New York, (1984).

[53] M. Jurna, J. P. Korterik, And H. L. Offerhaus, "Noncritical Phase-Matched Lithium Triborate Optical Parametric Oscillator For High Resolution Coherent Anti-Stokes Raman Scattering Spectroscopy And Microscopy", Journal of Applied Physics Letters 89, 251116 ,2006.

[54] Lithium Triborate (LiB$_3$O$_5$, LBO), Germany , [cited 2011 May 30], Available   from http://www.lasercomponents.com/de/suche/?q=lithium+triborate+
 05/11 / V2 / SB / divers-optik/laserstaebe_kristalle/lbo.docx

[55] László Pálfalvi, 2003, "Z-scan study of the nonlinear optical properties of LiNbO$_3$",Thesis , University of PÉCS.

[56] M. Sheik-Bahae, Ali A. Said, and E. W. Van Stryland, "High-sensitivity, single-beam n$_2$ measurements", Journal of Optics Letters ,Vol. 14, No. 17, PP 955,(1989).

[57] Eva Ule, 2015, "Measurement of The Nonlinear Refractive Index
by Z-scan Technique", University of Ljubljana, Slovenia , PP 4-5.

References

[58] T. Sivanesan, V. Natarajan , D. Jayaraman and S. Pandi, 2014 , "Third order Non- Linear optical properties of Vanillin Single Crystals by Z-Scan Technique", Scholars Research Library; 5 (4), PP16-21.

[59] M. Sheik-Bahae, Michael P. Hasselbeck, 2000, "Third Order Optical Nonlinearities", Chapter. 17, OSA Handbook Of Optics, New Mexico, Albuquerque, PP 27.

[60] Manuel R. Ferdinandus, 2014, "Techniques For Characterization Of Third Order Optical Nonlinearities", Thesis , University Of Central Florida, Orlando, Florida.

[61] Jean-Michel Ménard, Markus Betz, Iliya Sigal, and Henry M. Van Driel, 2007, "Single-Beam Differential Z-Scan Technique, Journal of Applied Optics", Vol. 46, No. 11.

[62] Amal F. Jaffar, 2012, "Optical Nonlinearity of Oxazine Dye Doped PMMA Films by Z-Scan Techniques", Journal of Al-Nahrain University, Vol.15 (2), June, pp.106-112.

[63] I. Fuks-Janczarek, R. Miedzinski1, M.G. Brik, A. Majchrowski,

L.R. Jaroszewicz, I.V. Kityk, Z-scan analysis and ab initio studies of beta-BaTeMo2O9 single crystal, Military University of Technology, Kaliskiego.

[64] Unnikrishnan K. P., 2003, "Z-scan and Degenerate Four Wave Mixing Studies in Certain Photonic Materials", Thesis, Cochin University of Science & Technology, India, PP.36,51.

[65] A. Acharya, R. Behera, G. S. Roy, "Non-linear characteristic of copper oxide (CuO) through Z-scan technique", Lat. Am. J. Phys. Educ. Vol. 6, No. 3, Sept. 2012.

[66] M. Sheik Bahae, Ali A. Said, Tai-Hue1 Wei,David J. Hagan And E. W . Van Stryland, "Sensitive Measurement Of Optical Nonlinearities

Using A Single Beam", IEEE Journal Of Quantum Electronics. Vol. 26. No. 4,760, (1990).

[67] M. H. MAJLES ARA, Z. DEHGHANI, "Measurement Of Nonlinear Responses And Optical Limiting Behavior Of TiO_2/Ps Nano-Composite By Single Beam Technique With Different Incident Intensities", International Journal of Modern Physics: Conference Series Vol. 5, 277–283, (2012).

[68] T. Sivanesan, V. Natarajan and S. Pandi, "Non-linear optical properties of α-glycine single crystals by Z-Scan technique, Indian Journal of Science and Technology", Vol. 3 No. 6, ISSN: 0974- 6846, 653,(2010).

[69] Manfred Wöhlecke, Klaus Betzler, Mirco Imlau , 2005,"Nonlinear Optics", Osnabrück , Germany, PP.68.

[70] Binoy Paul,2004,"Investigationsof nonlinear optical properties of certain organic photonic materials using Z-Scan and DFWM techniques, India, PP53.

[71] Omed Gh. Abdullah, Bakhtyar K. Aziz ,Dler Mohammed Salh , "Structural and Optical Properties of PVA:Na2S2O3 Polymer Electrolytes Films" , INDIAN JOURNAL OF APPLIED RESEARCH , Volume : 3 , 2013.

[72] Ahmed Ahmed, "Synthesis and Modified of Poly(Vinyl chloride) Contains Triazole Moieties and Studying the Optical Properties of New Polymers", Journal of Al-Nahrain University Vol.18 (1), 2015, pp.66-73.

[73] Aqeel Salah Fadhil Al-Moathen, 2009, thesis, "Study of Nonlinear Optical Properties of Olive Oil", AL Nahrain University, PP33.

Papers Publish

1. Study of the Nonlinear Optical Properties of Lithium Triborate Crystal by Using Z-Scan Technique.

Published in:

   " International Journal of Science and Research (IJSR)"

2. Study of the Second and Third Harmonics Generation in Lithium Triborate Single Crystal.

Published in:

   "International Journal of Science and Research (IJSR)"

الخلاصة

تم دراسة توليد التوافقيات و الخواص البصرية الخطية و اللاخطية في هذه الرسالة تجريبيا لتحسين أداء البلورة النقية الاحادية الليثيوم ثلاثي البورايت والتي أبعادها (٥,٩٥ × ٥,٩٥ × ٥,٩٥) ملم^3، كنموذج مقترح لتوليد مزيج من التوافقيات العليا باستخدام ليزر النديميوم ـ ياك الذي يملك طيف اساسي ذو طوال موجيه حوالي ١٠٦٤ نانومتر و ٥٣٢ نانومتر.

وضعت البلورة في جهاز طيف الاشعة المرئية و طيف الاشعة فوق البنفسجية UV-Visible (Spectrophotometer) حيث تم قياس طيف الامتصاصية و النفاذية و تم حساب معامل الانكسار الخطي و معامل الامتصاص الخطي من خلال طيف النفاذية عند الاطوال الموجية ٥٣٢ نانومتر و ١٠٦٤نانومتر.

كما درست الخواص البصرية اللاخطية باستخدام تقنية المسح على المحور الثالث باستخدام ليزر النديميوم ـ ياك (Nd:YAG) بطول موجي ٥٣٢ نانومتر و ١٠٦٤ نانومتر و بقدرات (٢٥ و ٤٠) ملي واط. حيث اجريت القياسات بتقنية الفتحة المغلقة ،التي استخدمت لقياس معامل الانكسار اللاخطي الذي وجد انه يساوي(٠,٦٢×10^{-9}ملي واط/ سم^2) عند الطول الموجي ١٠٦٤ نانومتر ذو القدرة (٤٠ ملي واط) و (٣,٠٤×10^{-9} ملي واط/ سم^2) ،(١,٨٥×10^{-9}ملي واط/ سم^2) عند الليزر ذو الطول الموجي ٥٣٢ نانومتر ذو القدرات(٢٥ و ٤٠ ملي واط) على التوالي.

استخدمت تقنية الفتحة المفتوحة، لقياس معامل الامتصاص اللاخطي و وجد انه يساوي (٢,٣×10^{-3}ملي واط/ سم) عند الطول الموجي ١٠٦٤ نانومتر ذو القدرة (٤٠ ملي واط) و (٣,٧×10^{-3}ملي واط/ سم)، (٢,٣×10^{-3}ملي واط/ سم) عند الطول الموجي ٥٣٢ نانومتر ذو القدرات (٤٠ و ٢٥ ملي واط) على التوالي.

اظهرت النتائج التجريبية والحسابات النظرية لتقنية الفتحة المغلقة ان بلورة الليثيوم ثلاثي البورايت تملك معامل انكسار موجب (التركيز الذاتي)، اما نتائج تقنية الفتحة المفتوحة فأظهرت ان البلورة ذات امتصاص مشبع عند الطول الموجي ٥٣٢ نانومتر.

و دراسة القدرة على انتاج التوافقيات من الدرجة الثالثة تم باستخدام ليزر النديميوم ـ ياك (Nd:YAG) الذي يملك مدى من القدرات ما بين (٩٠ ـ ١٣٠) ملي واط و تم الكشف عن اشارة التوافقيات باستخدام الكاشف (LASER Power Meter LP١)، وقد تم تحديد شدة التوافقيات في حالتين لليزر ذو قدرة (٨٠ و ٣٥ ملي واط). الحد الأدنى من الشدة (٧,٣٣ × ١٠⁹ ملي واط/ سم²) عند (١٥٧٢٦٩ ملي واط/ سم) و (١,٠٤ × ١٠⁹ ملي واط/ سم²) عند (٦٨٨٠٥ ملي واط/ سم).

باستخدام النتائج التي تم الحصول عليها تجريبيا، وجد بأن كفاءة التحويل لتوليد التوافقيات من الدرجة الثالثة والثانية والتي يمكن الحصول عليها من شعاع الليزر ذو الطول الموجي ١٠٦٤ نانومتر هي (٧٠٪ و٣٠٪) على التوالي، والتي تم الحصول عليها بتقنية المرحلتين تتفق جيدا مع قياسات الكاشف، حيث ان كفاءة التحويل لتوليد التوافقيات من الدرجة الثانية تساوي نصف كفاءة التحويل لتوليد التوافقيات من الدرجة الثالثة هذه النتائج مرضية جدا لاستخدام بلورة الليثيوم ثلاثي البورايت في توليد التوافقيات من الدرجة الثانية و الدرجة الثالثة عند الطول الموجي ١٠٦٤ نانومتر.

البحث في انجاز بلورة الليثيوم ثلاثي البورايت (LBO) لتوليد التوافقيات العليا في الليزرات

رساله مقدمه

الى مجلس كلية التربية ـ جامعة القادسية

و هي جزء من متطلبات نيل درجة الماجستير في علوم في الفيزياء

من قبل

زهراء صاحب شنون

بكالوريوس علوم في الفيزياء ٢٠١٣

بإشراف

أ.د. رعد شاكر عبيس النايلي   أ.د. خوله جميل طاهر

١٤٣٧ هـ   ٢٠١٦ م